Water and the Thermal Evolution of Carbonaceous Chondrite Parent Bodies

ROBERT E. GRIMM[1]

Department of Earth, Atmospheric, and Planetary Sciences, Massachusetts Institute of Technology, Cambridge, Massachusetts 02139

AND

HARRY Y. MCSWEEN, JR.

Department of Geological Sciences, University of Tennessee, Knoxville, Tennessee 37996-1410

Many carbonaceous chondrites have been aqueously altered within their parent bodies. From chemical and textural data on these meteorites and from studies of collision mechanics, we pose two hypotheses for the aqueous alteration environment. In the first model, alteration occurs throughout the parent body interior; in the second, alteration occurs in a postaccretional surface regolith. Both models are based on the assumptions of an initially homogeneous mixture of ice and rock and heating by decay of ^{26}Al. Under the interior-alteration model, linked bounds on the initial ice-to-rock ratio and ^{26}Al abundance are found that satisfy alteration temperatures derived from oxygen isotope studies. We find that water may play a strong role in controlling chondrite evolution by acting as a thermal buffer that allows substitution of low-temperature aqueous alteration instead of high-temperature recrystallization. Additional constraints imposed by the inferred water volume consumed by the alteration reaction and the total water volume that exchanged oxygen isotopes with host rocks are best explained if alteration occurred in a regolith. We show quantitatively how liquid water may be introduced there by hydrothermal circulation, by diffusion of vapor from below, or by venting due to fracture when interior pore pressures exceed the parent body strength. A sealed permafrost zone is not required to ensure insulation of water long enough for aqueous alteration. Retention of primordial ice is probably not limited by sublimation or by collisional comminution, but by shock vaporization. If large, C-type asteroids are representative of carbonaceous chondrite parent bodies, they may still contain significant quantities of ice. © 1989 Academic Press, Inc.

INTRODUCTION

Carbonaceous chondrites, though among the most chemically primitive materials in the solar system, have been nonetheless modified within their parent bodies. Aqueous alteration, in particular, has played an important role in the petrogenesis of CM and CI chondrites (Kerridge and Bunch

[1] Present address: Department of Geological Sciences, Southern Methodist University, Dallas, TX 75275-0395.

1979, McSween 1979). In the first attempt to understand the link between thermal evolution and aqueous alteration, Du-Fresne and Anders (1962) proposed a qualitative model for a carbonaceous chondrite parent body in which internal heating released water from preexisting hydrous minerals until a liquid zone extended to just below the surface. Aqueous alteration was thought to have occurred there, beneath an insulating permafrost, over a period of a few thousand years, with the retention of free H_2O on the parent object controlled by

PRECEDING PAGE BLANK NOT FILMED

subsolar sublimation of ice. More recent research on carbonaceous chondrites has not addressed the thermal driving mechanism for alteration, but has focused on the complex mineralogy of altered matrix and vein materials (Richardson 1978, Kerridge and Bunch 1979, Bunch and Chang 1980, Barber 1981, Mackinnon and Zolensky 1984, Tomeoka and Buseck 1985, 1988; McSween 1987, Fredriksson and Kerridge 1988, Zolensky and McSween 1988).

In this paper, we develop the first quantitative models for the thermal evolution of carbonaceous chondrite parent objects. The small number of recovered carbonaceous chondrites of course does not allow their histories to be uniquely deduced. Nevertheless, there are now sufficient data—in particular, oxygen isotopic constraints on temperature and water volume present during alteration (Clayton and Mayeda 1984)—to test some simple hypotheses quantitatively. In developing this approach, there are many assumptions that must be tested concurrently. A large part of this paper is devoted to laying such a foundation, so that the initial conditions and parameter choices may be justified for future modeling efforts.

In contrast to the approach taken by Du-Fresne and Anders (1962), we assume that these parent bodies were initially mixtures of ice and anhydrous rock. We argue that these are two likely alternatives for the parent body aqueous alteration environment and subsequent sample delivery, In the first model, the interior of a carbonaceous chondrite parent object is altered throughout, and samples are derived following subsequent catastrophic breakup. In the second model, carbonaceous chondrites are derived solely from regoliths, without sampling of the deep interiors. For interior alteration, bounds on parent body size, composition, and heat source magnitude are given consistent with constraints on inferred peak temperature and extent of alteration. The thermodynamic and transport properties of water are shown to exert a strong influence on these models. We present representative calculations showing the thermal effects of aqueous alteration reactions. Several mechanisms for introducing water into near-surface regions are illustrated for the regolith-alteration hypothesis, and we address the issue of long-term retention of ice on parent bodies. Finally, we discuss the remaining discrepancies between theory and observation, and we suggest revised models for the aqueous alteration environment of carbonaceous chondrites.

ALTERATION IN CARBONACEOUS CHONDRITE PARENT BODIES

Three important processes that affected early carbonaceous chondrite history were irradiation, brecciation, and aqueous alteration. Although many carbonaceous chondrites contain large amounts of "planetary" noble gases (Goswami et al. 1984), the occurrence of some "solar" gases and solar-flare tracks supports residence within regoliths during at least part of their history. Most, and possibly all, CM and CI chondrites are breccias. As such textures have been interpreted as indicating that these meteorites have been compacted in a surficial regolith, it is then important to ask if aqueous alteration, too, occurred in a regolith environment (Kerridge and Bunch 1979, Bunch and Chang, 1980).

Petrographic observations of carbonaceous chondrites (Richardson 1978, Kerridge and Bunch 1979, Tomeoka and Buseck 1988) indicate that phyllosilicate formation and filling of fractures by mineralizing fluids occurred in several stages, consistent with the idea that mineralization and impact brecciation were contemporaneous. However, earlier alteration in asteroidal interiors cannot be ruled out, as some observations of compositional variations suggest that aqueous alteration of matrix materials may have largely preceded mechanical reworking. For example, McSween and Richardson (1977) found that matrix compositions in CI chondrites are

fairly constant within individual breccia clasts but vary between different clasts; similarly, host and clasts in CM chondrites also have distinct compositions (McSween 1987). Moreover, Richardson (1978) was able to describe the compositions of vein mineralizing solutions by local leaching of preexisting matrix phyllosilicates, which suggests that filling of fractures postdated primary alteration.

From the isotopic evolution of Sr in CI carbonate, Macdougall *et al.* (1984) inferred that vein formation occurred very early, certainly within 100 my of the 4.55-by formation time of unaltered chondrites and possibly within 10 my. Fission-track compaction ages (Macdougall and Kothari 1976), representing the times at which altered phyllosilicate and isolated olivine grains came into final contact, range from 4.5 to 4.3 by for CM chondrites (Caffee and Macdougall 1988); individual ages are accurate only to within 100 my or so due to uncertainties in the initial $^{244}Pu/^{238}U$ ratio and the nature of the precompaction environment. Taken together, these measurements provide an approximate upper limit of a few hundred million years for the duration of brecciation and alteration.

Both brecciation and aqueous alteration of carbonaceous chondrites, then, must have occurred very early, either during or shortly after accretion, although the relative timing of these processes remains uncertain. Two broad classes of hypotheses that can account for aqueous alteration differ in the location of, and thus the heat sources and physical mechanisms involved in, the hydration of matrix minerals. In the first class, alteration may have occurred within planetesimal interiors with brecciation produced during accretion into parent bodies, or alteration may have taken place within the interiors of the final parent bodies with samples later excavated by catastrophic breakup. Scott and Rajan (1981) and Grimm (1985) have suggested similar models for the metamorphic history of ordinary chondrite parent bodies. In a compet-

ing class of hypotheses, brecciation and alteration may have taken place contemporaneously within a regolith. Because these processes occurred early in the history of the parent body, such a regolith could probably not be defined in the usual sense of a soil layer gradually excavated from underlying bedrock, but instead might include material above some depth to which the most recently accreted material was incompletely consolidated. These two classes of hypotheses may be termed interior alteration and regolith alteration, respectively.

The extent of alteration within a particular environment warrants further consideration. Carbonaceous chondrite parent bodies may have experienced pervasive aqueous alteration under either interior alteration or regolith alteration, with the result that these zones were largely petrologically homogeneous, or alteration could have been limited, such that these regions contained significant amounts of unaltered materials. Two lines of evidence that bear on this problem are asteroid collision mechanics and carbonaceous chondrite chemistry and texture.

Studies of asteroidal collisional histories (Davis *et al.* 1979, Housen *et al.* 1979) suggest that catastrophic impacts, which result in complete fragmention of a body, may have occurred repeatedly for most asteroids over solar system history, although the largest objects (diameters from 300 to 1000 km) probably experienced few, if any, such events (Greenberg and Chapman 1983). Most sizable asteroids gravitationally reaccrete following catastrophic collisions, but some mass fraction is lost. Although surficial rocks may be accelerated to greater velocities and preferentially escape during catastrophic collisions, it is likely that some samples from the asteroidal interior would also be ejected, especially over several episodes of fragmentation and reassembly. Moreover, the object may eventually be disrupted and its fragments dispersed. From these consider-

ations, we may reasonably infer that if a parent body has been totally shattered one or more times, then samples exist which show chemical and mineralogical features typical of conditions within the object's interior, if not representative of the entire range of conditions. Strong heterogeneity in the extent of alteration in an interior-alteration scenario, then, seems unlikely on the grounds that it is unreasonable that only altered carbonaceous chondrites would be delivered from a shattered parent body without any samples of other kinds of interior mineralogy, and no meteorites of the latter type have been reliably identified. This argument of course assumes that CM or CI chondrites are derived from different parent bodies than CO or CV chondrites. A homogeneously altered parent body offers the most straightforward way to sample a parent body interior and obtain only altered materials. In the context of this study, "homogeneity" implies only that similar processes occur throughout most of the parent body, so that petrographic and chemical signatures are comparable.

A regolith site for aqueous alteration may be excavated by either catastrophic or non-catastrophic collisions. Catastrophic events again raise the preceding question regarding sampling, leading to the identical conclusion that a homogeneous object is the most plausible condition. In this scenario, regolith alteration occurs within the broader context of interior alteration. Alternatively, carbonaceous chondrites may be "chipped off" by noncatastrophic events that sample only shallow depths of the parent object (i.e., normal impact cratering). If the parent object experienced only these kinds of events over the age of the solar system, the implied strength against fragmentation may be consistent only with a large asteroid. This argument may be challenged on the grounds that other mechanisms (such as location) may serve to shield a small object from disruption. Nevertheless, we will adopt this position for purposes of illustration, although

our conclusions do not exclusively require a large asteroid. Because the interior is unsampled in the regolith-alteration scenario, the composition of the parent body's interior is unconstrained.

The near one-to-one correspondence between petrographic type and chemical group among carbonaceous chondrites (i.e., the absence of unaltered and altered chondrites of the same group) argues further that processes which altered texture and mineralogy were pervasive, supporting either a fairly homogeneous object or a homogeneous regolith. In addition, although individual CM and CI chondrites are largely brecciated, they contain few unaltered materials. The exceptions are a few C3 clasts in Murchison (Olsen *et al.* 1988), a minor component that appears to have been a late addition from elsewhere after the bulk of Murchison was altered. Some chondrules and inclusions in CM chondrites also show a few alteration effects, but they have survived the alteration process largely intact.

The principal alternative models for the aqueous-alteration environment under consideration here, then, are that of homogeneous alteration of an object's interior, either in parent bodies or accreting planetesimals, or regolith alteration on a large object where the conditions at depth are unknown (Fig. 1). Of course, the comparatively small number of samples, and the presumably smaller number of parent body impact events responsible for their excavation, makes these hypotheses only the most likely out of a range of possibilities.

CONSTRAINTS ON THERMAL MODELS

Thermal models of ordinary chondrite parent bodies (e.g., Miyamoto *et al.* 1981) may be constrained to match peak temperatures inferred from the distribution of petrographic types among a particular chemical group, as well as cooling rates inferred from metallographic or isotopic closure methods. Among altered carbonaceous chondrites, differences in petrographic type
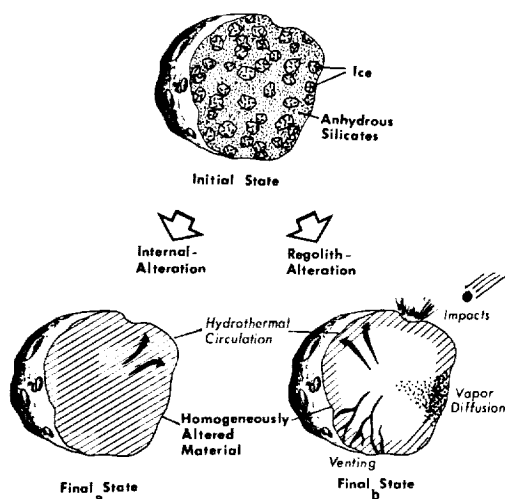
Fig. 1. Schematic illustration of the alternative models tested in this paper for aqueous alteration of carbonaceous chondrites. (a) Alteration occurs uniformly throughout the parent body interior. Hydrothermal circulation may develop at sufficiently large thermal gradients. (b) Alteration occurs within a regolith. Under internal heating, water may be supplied to the regolith by *in situ* melting and hydrothermal circulation, by venting through fractures that accompany tensile failure of the parent body interior at high fluid or gas pressures, or by simple vapor diffusion through preexisting pores and cracks. Impacts can also contribute to melting of ice within the regolith.

(2 versus 1) may indicate variations in the degree of aqueous alteration rather than variations in temperature (McSween 1979). Some temperature constraints are available for the carbonaceous chondrites, however, on a group basis. Moreover, hydrous : anhydrous mineral ratios and isotopically determined water : rock ratios provide additional constraints on prior history. Metallographic cooling rates, even if enough metal grains were present in altered carbonaceous chondrites, would not be a meaningful guide to parent body size or thermal history, because the low alteration temperatures lie below the metallographic closure intervals.

Alteration Temperatures

The "peak" temperatures experienced by CM and CI chondrites, while in contact with water, have been estimated by Clayton and Mayeda (1984). The strong oxygen isotope fractionation between calcite and hydrous matrix phases may restrict the temperature during aqueous alteration to 25°C or less for CM chondrites. At the present time it is difficult to judge the validity of this measurement as a peak temperature rather than a late-stage "quenching" temperature, but we have little choice but to treat it as an estimate of the conditions prevailing during alteration. Under the assumption that CI chondrites had an anhydrous precursor similar to that observed in CMs, Clayton and Mayeda (1984) derived a limiting alteration temperature of 150°C for CI meteorites. These are the only available temperature estimates for the alteration process although the higher temperatures inferred for CI chondrites may be inconsistent with the observation that CI phyllosilicates are more poorly crystallized than those in CM chondrites (Tomeoka and Buseck 1988).

These bounds are applicable only for the period during which rock was in contact with water; if water was later expelled or exhausted by chemical reactions, subsequent temperatures would have been free to rise. Rietmeijer and Mackinnon (1985) inferred that temperatures of approximately 190°C for CI and 260°C for CM chondrites were necessary to produce the observed ordering in poorly graphitized carbon. We do not know for certain that graphitized carbon was produced *in situ*. Moreover, these estimates are accurate only to within 100°C, and temperatures may also be systematically shifted to lower values by catalytic activity or long heating times. A better peak temperature constraint is imposed by dehydration of matrix phyllosilicates. Textures attributed to partial dehydration of serpentine-type phyllosilicates have been observed recently in two CM chondrites (Akai 1988), but these features may also represent incomplete hydration (Zolensky *et al.* 1989). Although the search for similar textures in other carbonaceous chondrites is incomplete, it is clear that

these meteorites did not experience temperatures significantly in excess of the dehydration interval, or else there would be no hydrous matrix phases. Akai (1988) experimentally reproduced the patchy, disordered, and defect structures observed in two Antarctic CM chondrites by heating samples of Murchison to 500°C for 1 hr. Such textures were not observed at 400°C. The short duration of these experiments, however, makes extrapolation to longer time scales uncertain. Instead, we adopt a value of 350°C as the value for the long-term dehydration temperature, based on measurements by Johannes (1968) of the equilibrium phase boundary for the reaction transforming serpentine and brucite to forsterite and water. We discuss this reaction further in a later section. A temperature of 350°C may then be taken as the limiting value for CI and CM chondrites following expulsion or exhaustion of H_2O.

The anhydrous CO chondrites are of course unconstrained by these arguments on aqueous alteration. Textural, mineralogical, and chemical studies limit the peak temperatures of this group to 450°C (McSween 1977).

Timing and Extent of Aqueous Alteration

The strontium isotopic composition of vein carbonate in CI chondrites (Macdougall *et al.* 1984) and compaction ages for CM chondrites (Macdougall and Kothari 1976) limit the alteration period to within a few hundred million years of accretion, and may require an even shorter period. Since we will argue below that the alteration reaction itself was rapid, this constraint applies principally to the duration of heat sources and the availability of water. It is assumed here that the entire matrices of CI and CM chondrites are composed of altered materials; the required volume factions v_h and v_a of hydrous and anhydrous minerals are then in the ratios $v_h/v_a \sim 1.0$ and ~ 0.5, respectively (Dodd 1981). CO chondrites are taken to be completely unaltered, so $v_h = 0$.

Water : Rock Ratio

In addition to alteration temperatures, Clayton and Mayeda (1984) also estimated water : rock oxygen mass ratios for aqueously altered carbonaceous chondrites. These ratios may be expressed as water volume fractions of 0.8 and ~0.5 for CI and CM chondrites, respectively. Such estimates correspond to the total volume of water flushed through a volume of rock over time, because no reasonable pore volume can hold 80% water. Therefore the water : rock ratios indicate H_2O transport for CI chondrites, and possibly for CM as well. Because not all of the water that moves throughout the asteroidal interior will exchange oxygen isotopes with the rock, we may assume that these water volumes are lower limits.

FORMULATION OF THERMAL HISTORY MODELS

Even within the restricted framework of the homogeneous interior alteration or regolith alteration models, uncertainty in the initial conditions generally prohibits a unique solution for all model parameters consistent with observational constraints. A series of interior-alteration models is examined below to test for acceptable combinations of size, water volume fraction, and heat source abundance that satisfy peak temperature and homogeneity constraints. We consider only qualitatively the constraints of water : rock ratios. We complete the interior-alteration investigations with some simple tests of aqueous alteration chemical reactions on parent body thermal history. For regolith-alteration models, our approach is of necessity more exploratory. By explicit models, we seek to test the viability of possible mechanisms for introducing water into such an environment under representative conditions.

In our basic model, carbonaceous chondrite parent bodies are taken to be initially cold mixtures of ice and anhydrous silicates heated by [26]Al and chondritic complements of long-lived radionuclides. When ice is

melted, water may react with the rock to produce hydrous silicates. The effects of latent heat are included for both H_2O and silicates. Dehydration is assumed to occur at 350°C. Under sufficiently large temperature gradients, hydrothermal circulation may develop, redistributing heat so the interior reaches an isothermal state. Gas diffusion occurs as temperatures rise and increasing amounts of H_2O are vaporized. At high pressures, the overlying rock will fracture, and H_2O will be vented into the regolith or to space. Although we have attempted to identify several important processes that may contribute to the thermal history of carbonaceous chondrite parent bodies, in practice not all elements of this model are evaluated simultaneously.

While the mathematical details of the thermal history models are given in Appendix A, supporting arguments for this model are presented in this section. We discuss separately those processes occurring before the period of aqueous alteration and those taking place during alteration. Among the former processes are nebular condensation, accretion, and lithification of carbonaceous chondrite parent bodies. Among the issues important for the alteration stage are the heat sources responsible for volatile mobilization and mild metamorphism, the permeability of parent bodies undergoing hydrothermal circulation and gas transport, and the rate of aqueous alteration.

Nebula Condensation

The equilibrium condensation sequence (Grossman 1972, Lewis 1972, Goettel and Barshay 1978) has provided a basis for understanding the radial compositional structure of the solar system. For potential aqueous alteration of carbonaceous chondrites, two crucial events were the formation of major H_2O-bearing phases such as serpentine and talc at $T < 400°K$ and the condensation of water ice at $T < 200°K$ (Lewis 1972). The radial distances at which these phases appear may be estimated from models of the pressure and temperature

structure of the solar nebula (Cameron and Pine 1973, Wood and Morfill 1988). Lewis' model shows the formation of talc in the region of the asteroid belt, whereas ice did not condense until nearly the distance of Saturn. By this model, hydrated silicates provided the original source of water in the region from Mars to Jupiter, including the putative asteroidal sources of meteorites. This assumption was implicit in the DuFresne and Anders (1962) model for carbonaceous chondrite parent bodies.

Chemical and isotopic evidence in carbonaceous chondrites for the nebular equilibration of dust and gas has been critically reviewed by Bunch and Chang (1980), who suggested instead that direct condensation of ice and its accretion into parent bodies was possible. Recently, Prinn and Fegley (1988) have questioned whether the equilibrium condensation assumption itself is valid, i.e., was chemical equilibrium reached within 10^5–10^6 years, the lifetime of the solar nebula? By simple thermokinetic arguments, Prinn and Fegley showed that formation of hydrous minerals under nebular conditions would require time scales $>10^{15}$ years for solid–solid reactions and 10^9–10^{10} years for gas–solid reactions. Even the more rapid case is 10^4 times longer than the lifetime of the solar nebula, providing a powerful argument that formation of primary hydrous minerals from the solar nebula at $T < 300°K$ may have been kinetically inhibited. On the basis of revised condensation and nebula models, Prinn and Fegley favored direct condensation of ice at the distance of the present-day outer asteroid belt. Considering the equilibration and thermokinetic arguments together, we assume that H_2O was incorporated into primary parent objects as ice instead of as an earlier generation of hydrous minerals.

The initial proportion of ice and its degree of mixing with rock depends on the relative timing of ice condensation and parent body accretion. We consider a homogeneous accretion scenario, so that ice and rock are initimately mixed throughout the

parent body. Dodd (1981) described carbonaceous chondrite matrix materials as "chemically unfractionated and the result of essentially complete condensation of nebular gas." It is not known, however, if this quenching extended to temperatures low enough for H_2O condensation, so that ice and rock would accrete together. Voids interpreted to have formed during evaporation of volatiles have been observed in the Orgueil CI chondrite (Tomeoka and Buseck 1988), but unambiguous textural evidence for the presence of ice–rock mixtures has not been found. An upper limit to the H_2O volume fraction of ~0.8 is given by cosmic abundances (Anders and Ebihara 1982); such high proportions of ice would be appropriate for comet-like objects formed at solar distances much farther than the asteroids. In this study, we limit the volume fraction of ice to 0.4 based on mechanical considerations (see below).

Accretion

We assume that accretion is rapid compared with interior heating, so that the initial temperature profile is uniform and equal to the surface value in equilibrium with insolation (impact heating during accretion is negligible). Because plausible heat sources have durations of 10^6–10^7 years (see below), accretion times must be shorter than these values if this assumption is to be valid. Numerical simulations of planetesimal accretion at 2.7 AU (Greenberg *et al.* 1978) show that objects several hundred kilometers in diameter may form within ~10^5 years. Recent revisions to this algorithm (Patterson and Spaute 1988) have resulted in a sharp upward revision of accretion times for the smallest objects, but the integrated time to accretion of large asteroids is relatively unaffected. On the other hand, analytical approaches (Safronov 1979, Wetherill 1980) predict ~10^7-year accumulation times for large asteroids. As an upper limit, asteroid accretion times are constrained by the growth time of Jupiter. By gravitational perturbations due to Jupi-

ter itself, or by the scattering of Jupiter-zone planetesimals into the asteroid belt, encounter velocities between asteroids were increased such that further accretion was halted in favor of fragmentation and dispersal (Safronov 1972, 1979). Numerical studies by Davis *et al.* (1979) suggest that interactions with Earth-sized, Jupiter-scattered planetesimals raise typical asteroid encounter velocities to 5 km/sec within 10^6–10^7 years. These calculations are based on the presumed preexistence of such planetesimals, which may themselves take ~10^8 years to accrete (Wetherill 1980); however, a runaway growth could occur here as well (Patterson and Spaute 1988). Since the time scale for accretion cannot be adequately resolved from the time scale for internal heating the assumption of short accretion times must be viewed as ad hoc. Isotopic limits to alteration times are still sufficiently imprecise that they cannot resolve the differences in accretion times considered here.

Following accretion, temperatures and compositional changes are assumed to be the result only of the internal evolution of the parent object. There is some evidence among ordinary chondrites, however, to suggest that internal evolution was contemporaneous with further accretion (Scott and Rajan 1981) or with collisional disruption and gravitational reassembly of the parent object (Grimm 1985). We address contemporaneous alteration and accretion by finding the lower limit in size for objects that can satisfy the appropriate peak temperature constraints.

Parent Body Compaction

It is assumed that carbonaceous chondrites are fully lithified throughout the history represented by these calculations, although the mechanisms that could lead to consolidation and lithification in meteorites, such as overburden (Cain *et al.* 1985), impact (Sugiura and Strangway 1983, Sneyd *et al.* 1988), thermal recrystallization (Yomogida and Matsui 1983, 1984), or pressure solution (Skinner 1989), are poorly un-

derstood. Most chondrites are coherent breccias in which clasts are also well lithified; the properties of these samples suggest that their parent bodies were well indurated. It is not known, however, if this induration was achieved before aqueous alteration. This assumption is critical, because if carbonaceous chondrites were still unconsolidated when H_2O was mobilized, differentiation of water and silicates may have occurred.

An upper limit to the rate of upward explusion of water from a rock skeleton may be specified if the silicates are completely deformable, so that pressures in the solid and fluid are the same. The separation velocity u is then given by Darcy's law, driven by a pressure proportional to the density difference $\Delta\rho$ between the two phases: $u = K\Delta\rho g/\eta$, where K is the permeability, g is the gravitational acceleration, and η is the viscosity of water. The Darcy segregation time $t_D \sim R/u$ is the characteristic time to move water over a length scale R. If the gravitational acceleration g is taken to be the average value by volume within a uniform sphere of radius R and density ρ, then $g = \pi\rho GR$, where G is the gravitational constant. With $\rho = 3$ Mg/m^3 and $\eta = 10^{-3}$ Pa-sec, we find $t_D \sim 10^{-13}/K$, expressed in millions of years. If this quantity is small compared with the characteristic thermal diffusion time for a sphere, $t \sim 0.1\ R^2/\kappa$, where κ is the thermal diffusivity, then water–silicate separation may occur. Since $\kappa \sim 10^{-6}$ m^2 sec^{-1}, the thermal diffusion and Darcy segregation times are comparable for $KR^2 \sim 10^{-4}$. At $K = 10^{-13}$ m^2, then, upward explusion of H_2O may begin at $R \sim 30$ km, with significant effects probably restricted to $R > 100$ km. However, the permeability is poorly constrained (see below) and could vary by two orders of magnitude in either direction. A more realistic treatment of the problem of fluid explusion from an elastic, deformable skeleton follows from soil consolidation theory (e.g., Lambe and Whitman 1969) but at the expense of introducing additional unknown parameters. We find no reason to reject hypotheses that H_2O expulsion by silicate compaction is either fast or slow. Our assumption that it is slow is largely for convenience in the present model, although we have considered the effect of complete water–rock differentiation on carbonaceous chondrite thermal history in a preliminary report (Grimm and McSween 1988); suggestions for future models with large water volumes are given under Summary and Conclusions, below. The maximum water volume fraction in the fully lithified case is then limited by the amount that will fit into the pores of a connected rock skeleton, approximately 40% by volume.

Heat Source

The heat source for primordial metamorphism and melting of meteorite parent bodies is still unresolved (Sonett and Reynolds 1979). However, two leading candidates have emerged: solar electromagnetic induction and the decay of the short-lived radionuclide ^{26}Al.

Electromagnetic heating of asteroids by the interaction of the early solar wind and solar magnetic field was first studied in detail by Sonett et al. (1970). A scenario constructed by Herbert and Sonett (1979) for anhydrous objects shows marginal silicate melting on Vesta but none on Ceres; this is principally caused by the inverse square falloff of spherically symmetric plasma flow and associated induction heating. The thermal histories inferred from the observed spectrophotometric structure of the asteroid belt suggest a heat source that diminished with solar distance (Gradie and Tedesco 1982, Bell 1986). However, there are a number of unknown model parameters associated with the physical state of the early sun, and an asteroid's response is sensitive to its electrical conductivity. Therefore, the extent of electromagnetic heating and uniqueness of model scenarios are difficult to evaluate quantitatively.

Aluminum-26 is the most favored of the potential short-lived radionuclides because

of its expected high abundance, high decay energy, and reasonably long half-life (Sonett and Reynolds 1979). Since the discovery of its decay product (excess ^{26}Mg) in Allende by Lee *et al.* (1976), numerous thermal models for meteorite parent bodies have been constructed using ^{26}Al as a heat source (see Basaltic Volcanism Study Project, 1981, for a review).

Because the ^{26}Mg excess was detected by Lee *et al.* (1976) only in refractory inclusions in Allende, the inferred initial abundance of ^{26}Al (initial ^{26}Al/^{27}Al $= 6 \times 10^{-5}$) may not be representative of the amount of ^{26}Al incorporated into parent bodies. In addition, it was immediately recognized by these workers that such levels of ^{26}Al would melt all but the smallest objects. Radiogenic ^{26}Mg had not been detected outside of refractory inclusions until Hutcheon *et al.* (1989) reported a ^{26}Mg excess in an anorthite-bearing chondrule in an ordinary chondrite, from which they inferred an initial ^{26}Al/^{27}Al of $(8 \pm 2) \times 10^{-6}$. The discovery of radiogenic ^{26}Mg outside of CAI's lends additional support to the hypothesis that ^{26}Al was incorporated into parent bodies. Although this new figure for initial ^{26}Al/^{27}Al may represent an upper limit, the value reported by Hutcheon *et al.* (1989) is not very different from that deduced from thermal models of ordinary chondrites. Under the assumption that the current collections of ordinary chondrites are representative samples of H and L chondrite parent bodies, Miyamoto *et al.* (1981) found that an initial ^{26}Al/^{27}Al of 5×10^{-6} for both objects would have been sufficient to explain the observed distribution of petrographic types and their inferred peak temperatures.

We believe that these modeling and experimental efforts support the case for ^{26}Al as a reasonable primordial heat source for chondrite parent bodies. The present model, then, is formulated in terms of radionuclide heat sources; however, the principal conclusions on the thermal evolution of carbonaceous chondrite parent bodies may not be markedly affected by choice of

heat source, because both ^{26}Al and electromagnetic induction operate on time scales of $\sim 10^6$ years and the internal temperature profiles produced by both sources are broadly similar (largely isothermal heating of the interior beneath a thin near-surface boundary layer; Sonett *et al.* 1970).

Since the heating requirements for aqueous alteration of carbonaceous chondrites are modest, mechanisms that have been ruled out for the heating of meteorite parent bodies—in particular, impacts—could apply here. Lange *et al.* (1985) have experimentally demonstrated that shock dehydration of serpentine occurs over the pressure interval 25–59 GPa. Such release of H_2O could be responsible for later secondary alteration and veining, but is not relevant to the melting of primordial ice required for primary alteration. Shock melting of ice occurs over the interval 8–10 GPa; the corresponding minimum impact velocities, appropriate for a rock projectile and an ice target, are ~ 3 km/sec (Chapman and McKinnon 1986). During the accretion period, encounter velocities are comparable to the escape velocity of the largest object in the population (Safronov 1972), which indicates that impact velocities between asteroids during accretion were only several hundred meters per second at most. Impact melting of ice is therefore not likely during accretion. Encounter velocities among asteroids were gradually raised to the present value of ~ 5 km/sec, however, by gravitational interactions with Jupiter or its scattered planetesimals. As described previously, both the inferred time scale for such planetesimal growth (Wetherill 1980, Patterson and Spaute 1988) and the time scale required to pump up asteroid velocities (Davis *et al.* 1979) only weakly constrain the time scale on which impact melting of ice can become effective to 10^6–10^8 years. Since accretion times are probably 10^5–10^7 years, it appears that impact melting can effectively melt ice in postaccretional regoliths. Most carbonaceous chondrites show only weak evidence of shock, which sug-

gests that they were not subjected to hyper-velocity impact. Unfortunately, the correlation of shock facies (Dodd and Jarosewich 1979, Sneyd *et al.* 1988) and shock pressure (Sears *et al.* 1984) established for ordinary chondrites cannot be used to estimate shock pressures for carbonaceous chondrites, because significant strain could be accommodated by ductile matrix or ice. The shock levels experienced by carbonaceous chondrites and the contribution of impact release of water to aqueous alteration are therefore open questions. Nevertheless, carbonaceous chondrites still require some additional heat source to explain mild static metamorphism of the CO group (McSween 1977).

H_2O Transport

When heating of the parent asteroid reaches several hundred kelvins, large internal redistributions of H_2O may occur due to evaporation of water in the deep interior, diffusion through the porous interior, and recondensation in a (comparatively) near-surface shell. In addition, under sufficient heating, pore water itself may become gravitationally unstable and undergo hydrothermal convection. Both of these processes are sensitive to the permeability, a quantity which is not reliably known.

Sugiura *et al.* (1984) measured the permeability of Allende (CV3) to be $\approx 10^{-15}$ m^2, a rather low value characteristic of terrestrial silt or clay (Lambe and Whitman 1969) but consistent with the fine texture of the matrix. In the field, however, and presumably in asteroids, permeability is sensitive to the presence of fractures, which may greatly accelerate rates of fluid transport. Bunch and Chang (1980) described CM chondrites as having textures similar to those of terrestrial hydrothermally altered tuffs and mafic rocks. A possible terrestrial analog to such rocks is the Waiora formation, a unit of pumice breccias and vitric tuffs 600–800 m thick in New Zealand's Wairakei hydrothermal region. Mercer *et al.* (1975)
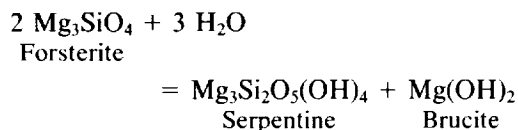
adopted $K = 10^{-13}$ m^2 (at observed porosity 0.2) for the bulk permeability of this unit, which includes the contribution from fractures. The volcanic rocks of the Waiora formation have larger grain (pore) sizes than the Allende matrix, so the bulk permeability of the Waiora formation probably will exceed that of Allende's parent body, unless the size and density of fractures between these two brecciated units vary substantially. The value 10^{-13} m^2 may be taken as a reasonable upper limit for the permeability of lithified asteroids. In the case of unlithified material, as discussed above, however, the permeability may have been as high as 10^{-11} m^2, an approximate upper limit for terrestrial sediments (Lambe and Whitman 1969). In addition, if the highly porous, silt-to-fine sand texture of the lunar regolith (Costes and Mitchell 1970) is any guide to asteroids, the near-surface permeability should lie in the range 10^{-11}–10^{-12} m^2.

If fluid or gas pressures exceed the sum of the rock's tensile strength and the lithostatic pressure, fracturing will occur and H_2O will be vented. Compressive strengths of equilibrated ordinary chondrites measured by Buddhue (1942) range from 62 bars to 3.7 kbar. From a typical ratio of compressive to tensile strength of 10 and typical tensile strengths of both sedimentary and crystalline rocks (Jaeger and Cook 1976), 100 bars (10^7 Pa) is taken as representative of the tensile strength of asteroidal interiors. Such a value implies that resistance to gas or fluid fracturing is dominated by the tensile strength (and therefore is approximately constant) for objects less than about 200 km in diameter; lithostatic pressure becomes increasingly important at larger sizes.

Rate of Aqueous Alteration

Aqueous alteration has profoundly affected the textures of carbonaceous chondrites, from millimeter-scale fractures to micron-scale matrix phyllosilicate grains.

DuFresne and Anders (1962) suggested that water was available for $>10^3$ years, on the basis of the ordering of dolomite crystals in CI chondrites. The actual aqueous alteration reactions in carbonaceous chondrites were complex, leading to hydrous minerals such as serpentines, septechlorites, and montmorillonites. In order to assess quantitatively the time scale for aqueous alteration, the reaction

$$2 \text{ Mg}_3\text{SiO}_4 + 3 \text{ H}_2\text{O}$$
Forsterite

$$= \text{Mg}_3\text{Si}_2\text{O}_5(\text{OH})_4 + \text{Mg(OH)}_2$$
Serpentine   Brucite

is taken to be representative of carbonaceous chondrite aqueous alteration. Both hydration and dehydration rates for this reaction were studied by Wegner and Ernst (1983), who give the time for 99% hydration of olivine as a function of fluid pressure, temperature, and grain size. Even at the low fluid pressures relevant to this problem, hydration of millimeter-size grains at 0°C will be complete in $\sim 10^4$ years. For the micron-size grains of carbonaceous chondrite matrices, hydration should take only about a year at 25°C (a possible upper limit to the alteration temperature inferred from isotopic studies, discussed above). Olsen *et al.* (1988) also concluded that the duration of carbonaceous chondrite aqueous alteration could have been short, $\sim 10^2$ years. Because aqueous alteration is fast compared with the thermal evolution time scales of asteroids, we may consider such reactions to be instantaneous in the context of thermal models. Although characterized by a different time constant, dehydration rates are also rapid (Wegner and Ernst 1983), due to increased thermal activation.

In these models we assume that the fluid phase is pure H_2O. On CM and CI parent bodies, mineralizing fluids had more complex chemistries, as evidenced by the fact that Ca–Mg–Fe carbonates and sulfates precipitated sequentially (Richardson 1978). Any kinetic effect of lowered activity of H_2O is ignored in these calculations.

RESULTS FOR INTERIOR-ALTERATION MODELS

Common parameters for both interior-alteration and regolith-alteration models are orbital semimajor axis 3 AU albedo 0.05, and emissivity 0.8 (estimated values for C-type asteroids). In order to obtain upper limits to hydrothermal convection, a reference permeability of 10^{-13} m^2 at saturated 20% pore volume is used.

Effect of H_2O on Peak Temperature and Limits on ^{26}Al Abundance

The following series of calculations demonstrates the primary effects of water on thermal evolution. The pore volume is taken to be saturated with H_2O; because this simplification easily leads to hydraulic fracturing at modest temperatures, venting of water is not included. Aqueous alteration and degassing are also neglected for purposes of these illustrations. The remaining variables are parent object diameter, water volume fraction, and initial $^{26}Al/^{27}Al$ ratio. In terms of these quantities, the problem may be formulated to find upper and lower limits to the radionuclide abundance at specified size and rock : ice ratio. The lower limit is that amount of ^{26}Al required just to melt water in the deep interior. Obviously, melting of a small volume fraction of the object will not expose much of its rock mass to water or lead to a homogeneously altered interior, but such a level of ^{26}Al may be regarded as a lower bound. The upper limit to ^{26}Al is constrained by the inferred peak temperature for each group described above. In order to estimate this bound conservatively for the homogeneous model, the volume-averaged peak temperature is used; core temperatures may be somewhat higher.

To provide some context for the magnitude of energy sources considered here, note that under perfectly insulating conditions, an initial $^{26}Al/^{27}Al$ ratio of 1×10^{-6} will result in a 200°K temperature increase if no H_2O is present. This change in temperature is limited to about 100°K if the initial
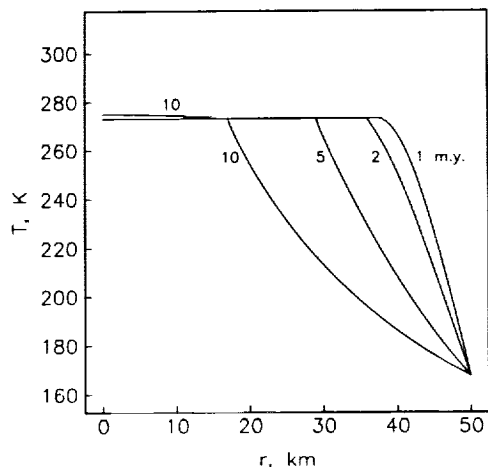
FIG. 2. Profiles of temperature versus radius within a parent body 100 km in diameter with 30% ice by volume and an initial ^{26}Al/^{27}Al ratio of 1.6 × 10^{-6}. The deep interior is brought just past H$_2$O melting in 10 my. This scenario gives the minimum heating required to produce interior aqueous alteration at the specified size and composition.

composition is 60% rock, 40% ice by volume. Furthermore, it takes an additional 0.4 × 10^{-6} initial ^{26}Al/^{27}Al at this composition to supply the latent heat of fusion of ice. Therefore, we can anticipate that the temperature increases of a few hundred kelvins required to attain carbonaceous chondrite hydration will require initial ^{26}Al abundances of several parts per million ^{27}Al.

The thermal history for an object 100 km in diameter and 30% ice by volume, which is brought just past the H$_2$O melting point by an initial ^{26}Al/^{27}Al ratio of 1.6 × 10^{-6}, is shown in Fig. 2. Following a rapid (<1 my) rise in temperature to the melting point, the interior remains so for several million years while the latent heat of fusion of ice is absorbed. Under this minimum-melting scenario, only a negligible volume in the asteroid's center rises a few degrees above freezing and is altered.

The thermal history of a similar object is given in Fig. 3, but with an initial ^{26}Al/^{27}Al ratio of 2.0 × 10^{-6}. Following H$_2$O melting, the central temperature rises to 310°K in

about 5 my. Water is gravitationally stable and no circulation occurs. The volume-averaged peak temperature of all rocks exposed to liquid water is 298°K (25°C), matching the required value for CM chondrites. However, less than half of the volume has melted—the outer 11 km stay frozen. This result illustrates a problem with constraining CM chondrites to small parent bodies: the bulk of the object must remain frozen in order to accommodate the narrow range of allowable temperatures, and the homogeneous alteration assumption is then violated. We return to this point below.

Figure 4a shows a similar calculation applicable to CI chondrites. An initial ^{26}Al/^{27}Al ratio of 4.3 × 10^{-6} results in melting of ice throughout 70% of the object's volume, and the mean peak temperature is 423°K (150°C). Hydrothermal convection has been suppressed in this calculation. Figure 4b shows a complementary model, also matching the CI alteration temperature (initial ^{26}Al/^{27}Al = 6.0 × 10^{-6}), in which hydrothermal convection is allowed. Circu-
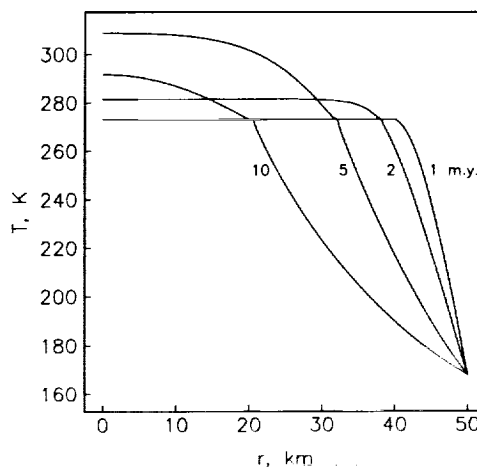

FIG. 3. Thermal evolution of an object similar to that in Fig. 2, but with initial ^{26}Al/^{27}Al = 2.0 × 10^{-6}. The average peak temperature of all rocks exposed to liquid water is 25°C, matching the alteration temperature of CM chondrites inferred from oxygen isotope studies (Clayton and Mayeda 1984). However, the altered rock fraction is not representative of the interior.
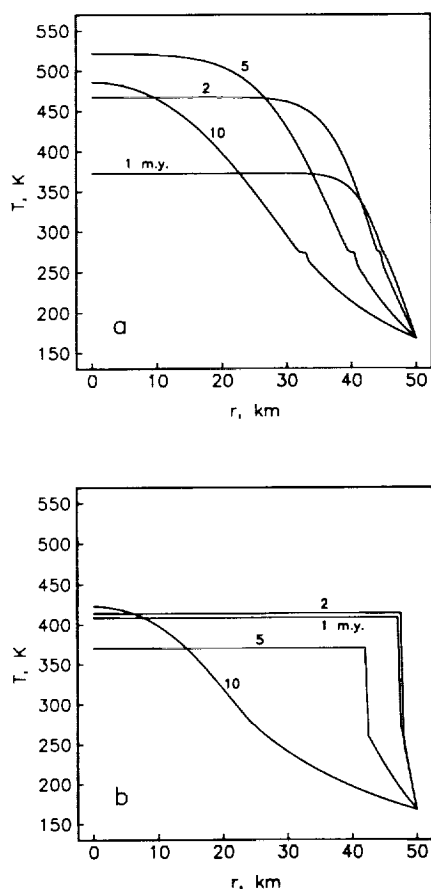
Fig. 4. Thermal evolution of an object similar to that in Fig. 2, but matching the CI inferred peak temperature of 150°C and illustrating potential effects of hydrothermal circulation. (a) Initial $^{26}Al/^{27}Al = 4.3 \times 10^{-6}$; convection suppressed. The altered fraction is representative of the interior. (b) Initial $^{26}Al/^{27}Al = 6.0 \times 10^{-6}$, with vigorous convection allowed so that excess heat is removed. The convective approximation overestimates the efficiency of heat transfer, so the indicated heat production is an upper limit at this size and composition.

lation of H_2O has a strong effect on the thermal evolution, homogenizing temperatures within the interior with the result that the object almost uniformly reaches the inferred peak temperature. Enhanced heat transfer allows melting of ice closer to the surface while suppressing strong temperature increases in the deep interior. Since the adopted approximation for convection

yields an overestimate of the heat transfer (Appendix A), Figs. 4a and 4b bound the range of thermal histories in a homogeneous CI parent body undergoing hydrothermal convection.

The calculations above have been repeated for a range of rock : ice compositions and object sizes. Results are summarized in Fig. 5. At a specified parent body diameter D, the lowermost curve gives the lower bound on ^{26}Al concentration, i.e., the level required just to melt ice. The next-higher curve gives the maximum initial $^{26}Al/^{27}Al$ which produces volume-averaged temperatures equal to the inferred CM peak temperatures, and the next corresponds to CI. Hydrothermal circulation does not develop in CM models, but it does for CI, and has been suppressed in this third curve as for the calculations in Fig. 4a. The uppermost, dashed curve gives the upper bound to ^{26}Al abundance, given generous assumptions on the efficiency of hydrothermal convection in CI objects. From Fig. 5, it can be seen that more ^{26}Al is needed, of course, to attain the same temperatures at a higher initial ice volume fraction. The radionuclide abundance must also be larger at smaller diameters to compensate for the increased heat loss. At $D = 1000$ km, required temperatures for all cases can be achieved by the decay of long-lived radionuclides alone, with the exception that a limited amount of ^{26}Al may be required in such a large CI parent body if hydrothermal convection is particularly efficient. The interval between minimum-melting and CM peak temperatures is smallest at $D = 100$ km because such objects are large enough to be insulating on the ^{26}Al decay time scale, but not on the decay time scale of K, Th, and U.

A calculation for anhydrous CO chondrites has also been carried out for each parent body diameter in Fig. 5. Since the observed porosity of carbonaceous chondrites is ~25% (Yomogida and Matsui 1983), the initial void volume fraction is taken to be 0.25 to illustrate the difference in thermal evolution between dry and H_2O-
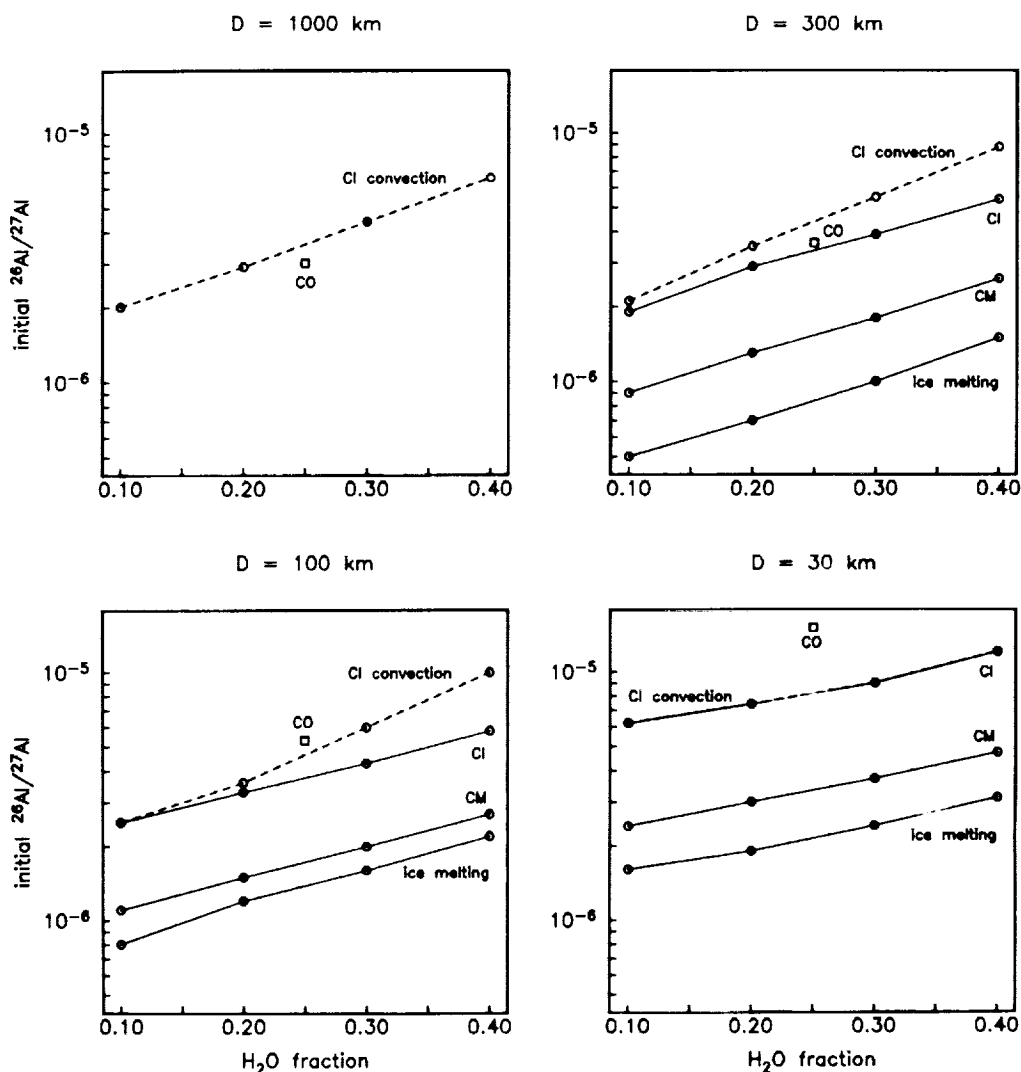
FIG. 5. Summary of allowed initial ^{26}Al/^{27}Al ratio as a function of parent body size, ice:rock composition, and carbonaceous chondrite group produced. In each panel, the lower curve gives the minimum ^{26}Al/^{27}Al required just to melt interior ice. The next two curves give initial ^{26}Al/^{27}Al ratios required to match inferred peak temperatures of CM and CI chondrites, respectively. The uppermost (dashed) curve gives an upper bound to ^{26}Al abundance in CI objects under efficient hydrothermal circulation; gravitational instability of water does not occur for CM models. Long-lived radionuclides alone are sufficient to heat a D = 1000 object to CI temperatures. Open squares give maximum initial ^{26}Al/^{27}Al ratios for anhydrous CO chondrites. Comparable ^{26}Al/^{27}Al ratios inferred for CI and CO chondrite parent bodies and also for ordinary chondrite parent objects (Miyamoto et al. 1981, Hutcheon et al. 1989) suggest that water may have played an important role in their different thermal histories.

saturated cases. The similarity of maximum radionuclide abundances between CI and CO chondrites suggests that water may play an important role in controlling their different thermal evolution; that is, water in CI chondrites may have acted as a thermal buffer to prevent the metamorphism experienced by CO chondrites. Moreover, the re-

quired initial $^{26}Al/^{27}Al$ ratios (several parts per million) are within the observational upper limit established for ordinary chondrites by Hutcheon et al. (1989) (8 × 10^{-6}), and reasonable agreement with the value inferred by Miyamoto et al. (1981) (5 × 10^{-6}) from thermal modeling of ordinary chondrite parent bodies can be found near D = 100 km. These arguments are more difficult to apply to CM chondrites, however, as their low inferred peak temperatures limit the initial $^{26}Al/^{27}Al$ ratios to a factor of 2–3 below those of CI parent bodies for the same diameter. If CM parent objects are smaller, more ^{26}Al can be accommodated, but at the expense of a smaller altered fraction of the interior.

These models explicitly satisfy inferred peak temperature constraints only. It is possible also to consider, but only qualitatively, the water:rock ratio derived from oxygen isotope data. Because hydrothermal circulation does not develop in homogeneous CM objects, the bulk water content must be at least 50% by volume, a value beyond those considered here. This is a lower bound, because exchange of water between liquid and silicates during aqueous alteration has been neglected in these calculations. Because of the greater range in temperature for CI chondrites, hydrothermal circulation is more likely, and hence it is possible that the time-integrated water:rock ratio for some samples could be large.

Finally, the presumption of interior homogeneity must be tested. We assume that at least 50% of interior rocks must be exposed to liquid water, in order for delivered samples of altered carbonaceous chondrites to be representative of the later-disrupted parent body. CM models satisfy this constraint at D = 300 km but do not at D = 100 km. For CI models without hydrothermal circulation, D = 100 km may be accepted, but D = 30 km is marginal. At large diameters, melting extends closer to the surface for water-convecting interiors than for nonconvecting ones. However, there is not much difference for smaller sizes, and so CI models with hydrothermal circulation at D = 30 km still produce ~50% altered rocks. Therefore, in addition to the restrictions on initial ^{26}Al specified by Fig. 5, homogeneous interior-alteration models may be constrained to parent bodies a few hundred kilometers in diameter and larger for CM chondrites and several tens of kilometers in diameter and larger for CI objects.

We described earlier a scenario in which interior alteration occurred in planetesimals before incorporation into parent bodies. Such a model may be excluded for CM chondrites because of the large object diameters required for homogeneous alteration, although accretion of smaller CI planetesimals is plausible.

Thermal Effect of Aqueous Alteration

In the preceding models, we neglected H_2O chemical exchange in order to demonstrate the thermophysical effects of the presence of the liquid phase alone. Three calculations are given here in the context of interior-alteration models to illustrate the potential effects of chemical reactions. Since little gas diffusion occurs below 273°K, degassing is again neglected, but finite strength against gas fracture is included. Figure 6a shows temperature profiles in a minimum-melting scenario for a 100-km-diameter objected heated at an initial $^{26}Al/^{27}Al$ ratio of 1.2 × 10^{-6}. The object's porosity is 20% and is saturated with H_2O. Melting of ice occurs over about a 3-my interval. Since aqueous alteration is rapid, hydrous minerals are effectively formed instantaneously. The final hydrous:anhydrous mineral ratio is ~1 (comparable to that observed in CM chondrites), and essentially all of the water at depth is exhausted by the reactions (Fig. 6b). The temperature in the deep interior increases markedly (~150°K) due to the substantial heat of reaction released, but the peak temperatures are well below those at which dehydration or thermal recrystallization would occur. Because of the speed of the
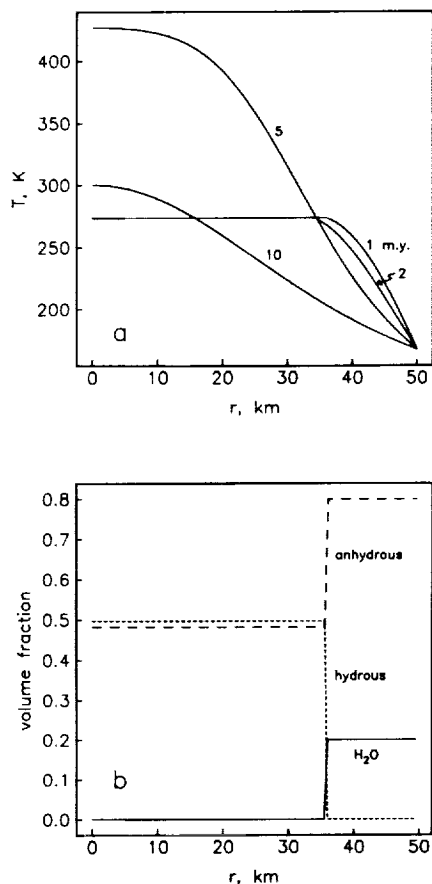
FIG. 6. Evolution of a CM object (D = 100 km, ice fraction = 0.2, initial $^{26}Al/^{27}Al$ = 1.2 × 10^{-6}) explicitly including thermal and compositional changes associated with aqueous alteration. (a) Temperature profiles. Following complete absorption of the latent heat of fusion of H_2O, temperatures increase sharply due to release of chemical heat of reaction. Oxygen isotopic constraints apply only during aqueous alteration, so peak temperature is limited instead by inferences from carbonaceous chondrite textures. (b) Compositional profile following alteration, showing volume fractions of H_2O (solid line), anhydrous minerals (long dash), and hydrous minerals (short dash). Hydrous: anhydrous mineral ratio matches CM proportions, but the altered zone is confined to the deep interior in this example.

reaction, the peak temperature during alteration is taken to be ~0°C, although in reality heat release from progressive alteration might cause substantial temperature excursions while liquid water is still available. As

a minimum-melting scenario, this CM model also suffers from a paucity of rocks exposed to water. However, because the oxygen isotope temperature constraints do not apply if water is rapidly removed by aqueous alteration, higher heat source concentrations would push outward the radius of the melting zone.

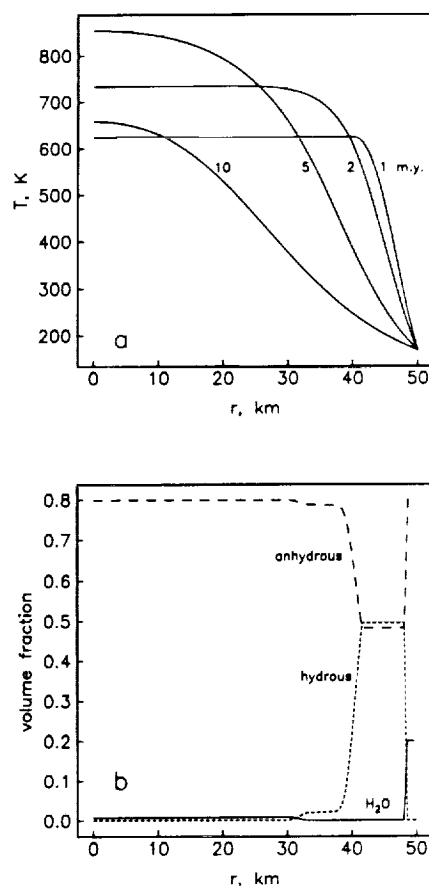As core temperatures reach 623°K (350°C), dehydration occurs. Figures 7a

FIG. 7. Evolution of an object similar to that in Fig. 6, but with initial $^{26}Al/^{27}Al$ = 5 × 10^{-6}. (a) Temperature profiles, showing rapid rise through hydration at 273°K to dehydration temperature (623°K) and maintenance of near-constant value during absorption of the latent heat of reaction. High pore pressures due to release of superheated water lead to failure of the surrounding rock and venting of H_2O. (b) Final compositional profile. Venting of H_2O following dehydration of the deep interior leaves only anhydrous minerals there. The altered zone is restricted to a depth of 1–11 km.
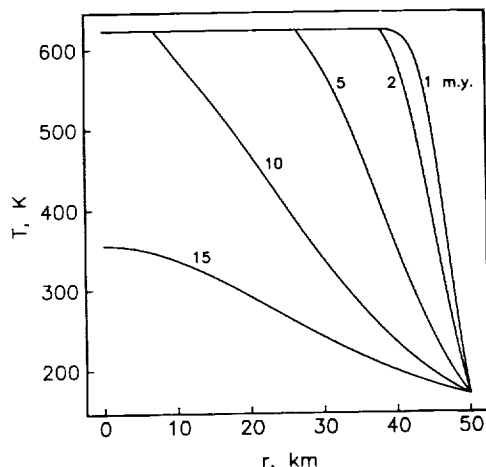
FIG. 8. Object with the same size and initial $^{26}Al/^{27}Al$ ratio as those of Fig. 7, but with initial H_2O doubled (volume fraction = 0.4). Such an H_2O fraction is needed to achieve the nearly complete alteration of anhydrous minerals observed in CI chondrites. Heating is insufficient to drive dehydration reaction, so dehydration temperature can act as a barrier to further temperature excursions. The final state (not shown) consists nearly uniformly of altered minerals, although in reality partial dehydration textures would be evident.

and 7b show temperature profiles at several times and the final composition profile at 10 my, respectively, for a similar object with an initial $^{26}Al/^{27}Al$ ratio of 5 × 10^{-6}. Melting of ice, aqueous alteration, and initiation of dehydration all take place within 1 my. The model parent body history becomes rather violent when dehydration reactions occur, because the pore volume is suddenly filled with near-critical H_2O. Since the pressure in the deep interior is several kilobars, immediate H_2O venting of the interior ensues, guaranteeing that rehydration cannot occur when temperatures again fall below 350°C. In the end, anhydrous minerals again dominate half of the volume, and the altered zone is restricted to depths between 1 and 11 km. As discussed above, there is no evidence for widespread dehydration among CM chondrites. Furthermore, oxygen isotope systematics preclude rehydration at a temperature as high as 350°C, even if H_2O

were not vented from the parent body interior.

A similar calculation (D = 100 km, initial $^{26}Al/^{27}Al$ = 5 × 10^{-6}) for CI chondrites is shown in Fig. 8. The highest water volume fraction allowed (0.4) is needed to achieve near-complete alteration of the anhydrous rock. The heat of reaction released is sufficient to send the temperature to the dehydration point, but not through it. In this example, the dehydration reaction is a barrier to further temperature excursions.

RESULTS FOR REGOLITH-ALTERATION MODELS

The release of liquid water occurs readily in interior-alteration models because of the insulating effects of overlying rock. In a cold surface regolith, however, supplying liquid is more difficult. We have conducted several thermal history calculations for internally heated parent bodies to illustrate the mechanisms by which liquid water may reach near-surface regions. The possible extent of impact melting within a regolith is briefly discussed.

To what depth does regolith alteration extend? Housen et al. (1979) numerically modeled regolith formation on asteroids and concluded that typical regolith thicknesses are a few kilometers or less. However, such regoliths develop over the age of the solar system (or until the object is disrupted), a condition that does not apply to the early regolith in which carbonaceous chondrites may have been altered. An upper limit to the thickness of such an accretional regolith may be estimated by considering the depth of the crater resulting from the largest possible impact that does not disrupt the asteroid. This depth is derivable in principle from energy and momentum considerations (Greenberg et al. 1978, Chapman and McKinnon 1986). A simpler approach is just to use the largest crater depth observed for small bodies (e.g., Herschel on Mimas), which suggests that impact turnover could extend to a depth of several kilometers. We therefore accept as

equally likely any internal heating model which supplies water to within such a distance of the surface. Even if liquid water reaches only the base of the regolith, impact stirring may allow access to upper levels.

Internal Heating

Water may be introduced into the regolith by internal heating in three ways: by direct melting of local ice, which may lead to H_2O circulation and replenishment from below, by venting of liquid or vapor along fractures caused by failure under high pore pressure, or by vapor diffusion through existing pores and cracks. Following the arguments given earlier that regolith-derived carbonaceous chondrites may require a large parent body, we give several models at $D = 300$ km which illustrate these mechanisms. Representative values in all cases for the initial $^{26}Al/^{27}Al$ ratio, porosity, and water volume fraction are taken as 5×10^{-6}, 0.25, and 0.1, respectively.

Figure 9a shows the thermal evolution of such an object in which hydrothermal circulation is suppressed. Melting of ice occurs deeper than about 3 km. However, gas pressures lead to venting of H_2O after about 1 my, which rapidly results in 70% water loss from the object (Fig. 9b). This water is removed from the calculation but is equivalent to a saturated surface layer 17 km thick. Therefore fractures initiating at depth can supply large quantities of steam of the regolith; condensation there would provide a low-temperature environment for aqueous alteration. Condensation must occur at least for the late veining, as CI textures imply that volatiles responsible for fracture filling must have been in the fluid phase, rather than as gases (S. M. Richardson, quoted in Kerridge and Bunch 1979).

Figure 10 illustrates a calculation identical to that of Fig. 9, but with hydrothermal convection. Beginning after 0.4 my, vigorous circulation and rapid heat losses hold down internal temperatures such that gas pressures achieve only minor venting.
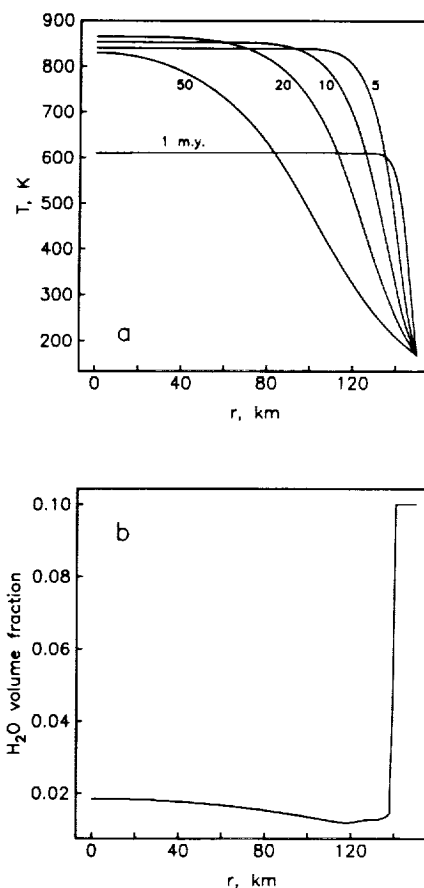

Fig. 9. Aqueous alteration within the regolith of a large ($D = 300$ km) parent body with initial $^{26}Al/^{27}Al = 5 \times 10^{-6}$, but the pore volume of 25% is taken to be undersaturated with only 10% H_2O. Hydrothermal circulation and chemical reactions are not included. (a) Temperature profiles. If only regolith is sampled, the high internal temperatures are irrelevant. (b) Final H_2O distribution. Large internal gas pressures cause failure of the surrounding rock, leading to venting of 70% of the object's H_2O. If part of this vented H_2O condenses in the regolith, a favorable environment for aqueous alteration would be provided.

Melting of ice, however, extends even closer to the surface (1 km) than in the previous example, well within our suggested accretional regolith.

Last, an example of gas diffusion is given in Fig. 11. This transport mechanism has been unimportant in models given heretofore because of subboiling liquid-saturated states, homogenization of H_2O distribution
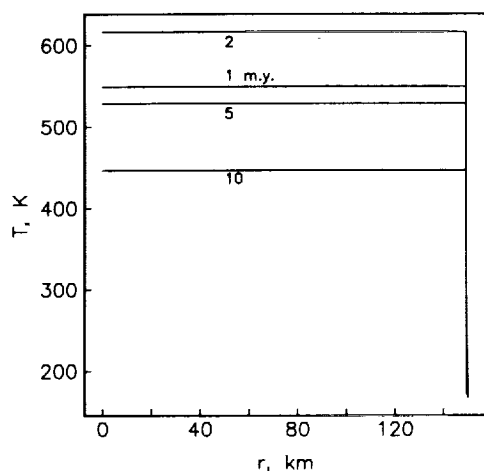
Fig. 10. Regolith-alteration calculation following that in Fig. 9, but allowing hydrothermal circulation. Vigorous convection holds down temperatures in the interior so that only minor venting of H_2O occurs. Melting also extends to within 1 km of the surface, closer than in Fig. 9. Regolithic water is continuously recharged by hydrothermal circulation.

by hydrothermal convection, or exhaustion of water by chemical reactions. In the case shown, hydrothermal convection is suppressed so that the H_2O distribution is not homogenized. Under diffusion alone, water vapor is depleted from the deep interior and deposited in the outer 10 km, perhaps within the depth of impact gardening, in the short span of 1 my.

Therefore under different initial conditions, direct melting and circulation, venting, and vapor diffusion all appear to be capable of satisfying the requirements of regolith alteration powered by internal heating. Although we favor a large object for this model, our calculations show that diffusion and venting can also operate on small ($D = 30$ km) parent bodies. Hydrothermal circulation into the regolith is not likely on small objects, because the temperatures at depth required to sustain such convection (which are minimum values under our approximation) would lead to silicate melting in the interior.

DuFresne and Anders (1962) suggested

that the expansion of freezing H_2O would form a sealed icy layer, beneath which an "internal atmosphere" could persist long enough for aqueous alteration to take place. Such effects could be important in sealing cracks formed when the interior fails under high pore pressure. We note, however, that the low temperature near the surface and the finite permeability of rock can strongly inhibit volatile loss (Fig. 11; also see Appendix B). The outermost layers of the parent body, then, can form a natural barrier to
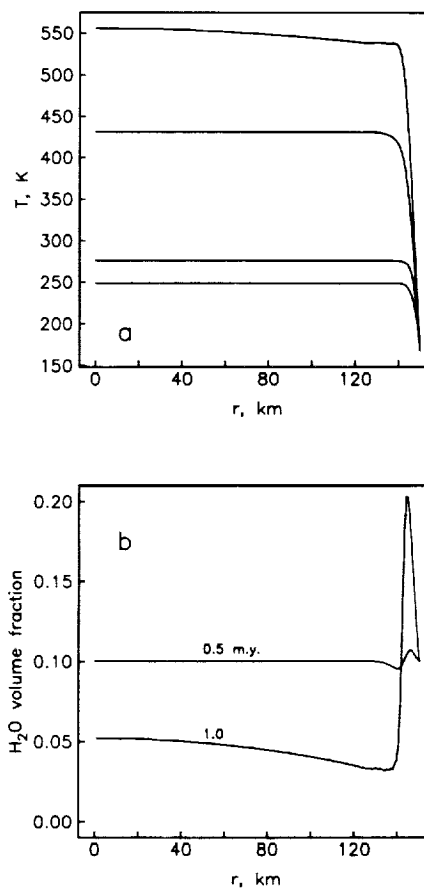

Fig. 11. Regolith-alteration model following that in Fig. 9, but including H_2O vapor diffusion. (a) Temperature profiles. (b) H_2O distribution. Hydrothermal convection must be suppressed or else water distribution is homogenized. The upper 10 km has a steady supply of vapor over time scales of ~1 my providing an additional mechanism for introduction of water into the regolith.

diffusion, provided that the rate of impact turnover is not too high.

Impact Heating

As discussed above, impacts are insufficient to shock-melt ice during accretion but become more effective when asteroid encounter velocities increase via gravitational interactions with Jupiter or its scattered planetesimals. Safronov (1978) and Kaula (1979) have studied impact heating of the Earth and Moon during accretion. A similar accretional-heating model for aqueous alteration of carbonaceous chondrites is conceptually simple, but the heat source has five free parameters (number of impactors as a function of diameter, velocity, and time; length scale for heat deposition and fraction of impact heat buried) as opposed to the single free parameter (initial $^{26}Al/^{27}Al$ ratio) required for radionuclide heating. Here we can at least compare the time scales for heat and volatile loss under an impact-heating hypothesis with the time scale required for aqueous alteration. The characteristic cooling time t at a depth z is given by $t \sim z^2/\kappa$, where κ is the thermal diffusivity. Given $t \leq 10^4$ years for aqueous alteration (see above) and $\kappa \leq 10^{-6} m^2 sec^{-1}$ (a typical value for solid rock) for regolith, then $z \leq 1$ km. At shallower depths, smaller values of t or κ are required to accomplish alteration, but there are no restrictions at greater depths. Using simple models for the distribution of impact heat with depth (Kaula 1979, Bratt et al. 1985), we find that that typical postaccretional impacts can easily melt ice to a depth of several kilometers. Therefore it appears likely that impact heat can be retained at depths of a few kilometers for sufficiently longer than the alteration time scale.

The limiting process, then, for impact-induced aqueous alteration must be loss of H_2O caused both by the initial shock of impact and by diffusion through highly fractured target rocks. Detailed modeling of these processes is beyond the scope of this paper, but arguments similar to those given below on the secular retention of ice in parent bodies suggest that both of these processes could rapidly deplete H_2O at shallow depths.

RETENTION OF H_2O IN CHONDRITE PARENT BODIES

Since we have expanded upon suggestions that ice may have been the original form of H_2O incorporated into parent bodies (Bunch and Chang 1980, Prinn and Fegley 1989), it is worthwhile to consider the long-term fate of H_2O in possible asteroidal sources. If aqueous alteration, degassing, or venting is not sufficient to deplete such objects of H_2O during primordial heating, then volatile loss occurs gradually over solar system history, and some fraction of the initial H_2O within meteorite parent bodies may still be present.

Appendix B presents a simplified treatment of the near-surface degassing problem, and gives a relation (Eq. (B7)) for the present depth of H_2O loss as a function of permeability and orbital semimajor axis. It should be recognized that this permeability is the *effective* value, including any potential effects of free molecular flow, as discussed in Appendix A. Solving (A17) for pore sizes of 1 mm and 1 μm, the transition temperatures to Knudsen flow are found to be 250 and 385°K respectively. Since the latter value is significantly above the $\sim 160°K$ surface temperature at 3 AU, free molecular flow can greatly enhance near-surface degassing. The depth of H_2O loss is plotted as a function of permeability for a pore size of 1 mm in Fig. 12a, and for a pore size of 1 μm in Fig. 12b. Because the pore size used is the smallest likely value, Fig. 12b gives conservative upper limits to the depth of H_2O loss.

At 3 AU, degassing is extremely slow even under the most conservative assumptions, so any primordial ice should still be retained. These results contrast sharply with predictions by DuFresne and Anders (1962) that sublimation should limit the lifetime of ice on meteorite parent bodies to
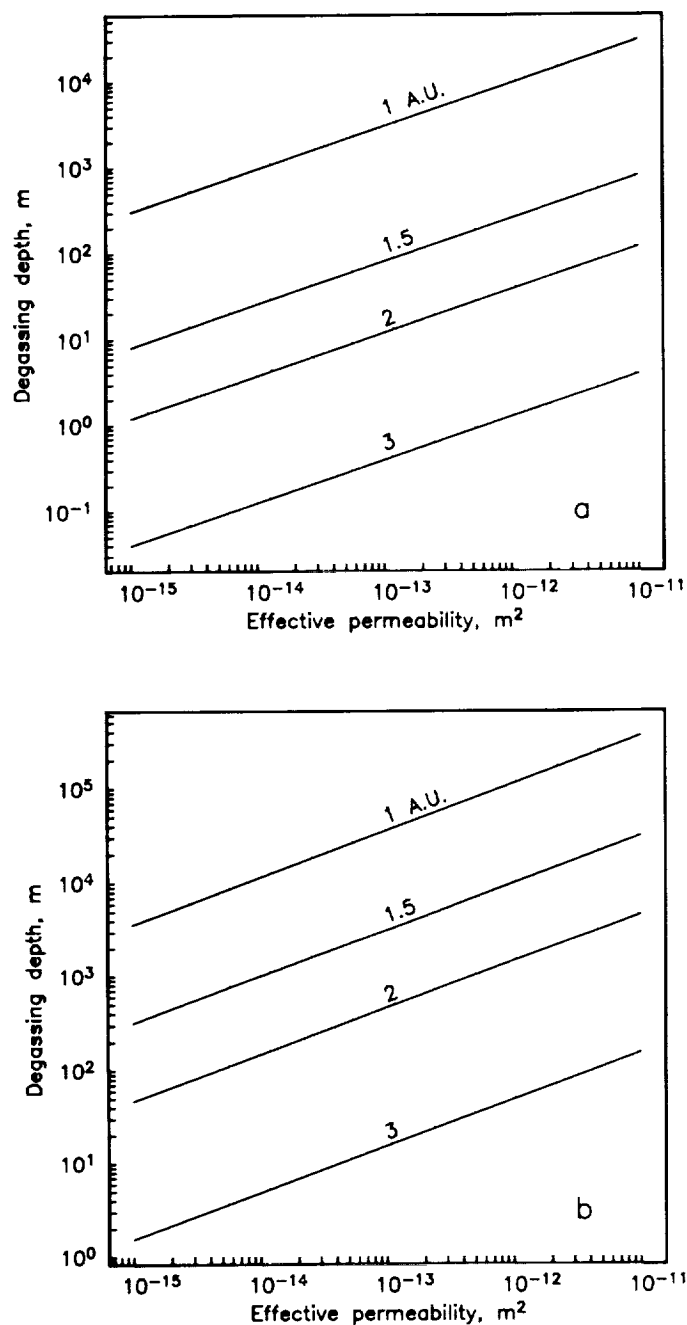
FIG. 12. Depth of H_2O loss over the age of the solar system as a function of reference permeability, for different values of solar distance. Effective permeability may be enhanced by low-temperature molecular flow and depends on pore size. (a) Pore diameter 1 mm, appropriate to the sizes of chondrules and clasts in carbonaceous chondrites. (b) Pore diameter 1 μm, appropriate to the size of carbonaceous chondrite matrix particles. For a fixed permeability, easier transition to molecular flow occurs for smaller pores, allowing greater H_2O loss. Degassing at asteroidal distances is nevertheless limited to depths of tens of meters.

only a few million years. Several geochemical observations might be interpreted as providing support for slow degassing, although other mechanisms could be responsible for these observations. Disturbances to the $^{87}Rb-^{87}Sr$ system (Mittlefehldt and Wetherill 1979) in some carbonaceous chondrites suggest that these meteorites were leached of Rb as late as 1 by after their formation, and the smooth $^{39}Ar-^{40}Ar$ release pattern in Murchison (Dominik and Jessberger 1979) indicates that gas was gradually lost from this CM meteorite at low temperatures.

Collisional evolution is an additional process that may result in more rapid H_2O loss. Collisions will cause H_2O loss both by an increase in surface area due to comminution and by shock vaporation. The loss due to comminution is probably small, for two reasons. First, the observed size distributions in both asteroids (Veeder 1986) and laboratory fragmentation experiments (Hartmann 1969) indicate that mass is concentrated in larger objects, so that a typical volume is well shielded. Second, most large asteroids probably reaccrete within a few orbital periods of fragmentation, and perhaps within times as short as a few days (Grimm 1985). Such short exposure times will further minimize the surface area available for H_2O loss. It is more difficult to evaluate the contribution of shock vaporization. Using impedance-match calculations tabulated by Kieffer and Simonds (1980), typical present-day asteroidal collisions should result in stress levels of a few tens of gigapascals over a length scale comparable to the size of the smaller asteroid (projectile). Since impact vaporization of ice occurs at pressures less than 20 GPa (Chapman and McKinnon 1986), it is apparent that the projectile can be completely devolatilized, as can two comparable-size bodies.

These considerations imply that large, primitive asteroids, e.g., Ceres, are particularly attractive candidates for primordial ice retention because they have undergone fragmentation and reassembly at most a few times, if ever (Davis et al. 1979, Greenberg and Chapman 1983). Using Fig. 12b as a guide, we suggest that such objects should still have ice accessible within tens of meters of the surface if impact stirring is minimal. Accumulation of a blanketing regolith, perhaps with a thickness of 1 km (Housen et al. 1979), would further insulate primordial ice over much of the asteroid. Slow loss of vapor from the interior might leave thin films of frost on the surface, as inferred from spectrophotometric observations of Ceres (Lebofsky et al. 1981, Jones et al. 1988).

SUMMARY AND CONCLUSIONS

A number of different processes relevant to the physical and thermal evolution of carbonaceous chondrites have been investigated here. We first present a brief summary of our approach (roughly parallel to the main sections of the paper), and then turn to discussion of the principal results.

Two hypotheses for the aqueous alteration environment have been investigated. In the first, alteration occurs throughout the interior of the parent body; samples are subsequently derived by catastrophic disruption of the object. In the second model, alteration occurs in an accretional regolith; samples are derived by cratering of the regolith and the interior composition is unknown.

We have considered the effects of nebula condensation, planetesimal accretion, parent body compaction, primordial heat sources, transport of H_2O, and aqueous alteration on the evolution of carbonaceous chondrites. The principal quantitative constraints (temperature and water volume) on the thermal models are derived from oxygen isotopic studies.

Tests of the interior-alteration hypothesis have been divided into models that explicitly include composition and temperature changes associated with aqueous alteration and those that do not. Regolith-alteration models alternatively consider internal and

impact heating. Finally, we examined the loss of primordial ice in parent bodies over the age of the solar system.

The results of interior-alteration models illustrate the potentially important role of H_2O in the divergent thermal histories of CI versus thermally metamorphosed CO and ordinary chondrites. Radiogenic heating can be buffered by the latent heat of fusion and large heat capacity of water, and by enhanced heat loss under hydrothermal convection. Therefore low-temperature aqueous alteration can occur instead of thermal recrystallization at the same heat source abundance. Hydrothermal convection may also be important in homogenizing interior temperatures and attaining locally high water:rock ratios inferred for CI chondrites from oxygen isotope studies.

The CM group is difficult to reconcile with the homogeneous interior-alteration hypothesis, however. At the same ^{26}Al levels inferred for other chondrites, the CM parent body must be small enough to lose heat rapidly in order to maintain low temperatures imposed by oxygen isotope data; in this case strong temperature gradients preclude a homogeneously altered interior. Because convection does not develop in the model CM objects, even under the generous assumptions used, there can be no local water:rock enhancement, and so the interior-alteration model might plausibly be rejected for this meteorite group.

The present treatment of aqueous alteration is undoubtedly oversimplified. Since complete reaction occurs immediately, but only after total melting of ice, water is never free to circulate. Consequently, there is no opportunity to satisfy constraints on water:rock ratios. In reality, melting and alteration might be contemporaneous. Heterogeneity in alteration reactions and significant convection velocities could allow water to circulate without reacting (cf. terrestrial hydrothermal zones).

If alteration occurred in regoliths, some additional inconsistencies may be qualitatively understood. Water can be introduced in great quantities from below by venting or vapor diffusion, but probably at irregular intervals, and removal of reaction heat is more easily accomplished from a near-surface location. Alteration by local melting of ice still fails to satisfy observed water:rock ratios, unless hydrothermal circulation extends into the regolith. Some fluid-transport mechanism is required to supplement the original DuFresne and Anders (1962) model. Aqueous alteration by impact heating faces a similar problem, in that there is no H_2O enhancement over the bulk composition of the regolith and the projectile population, unless impactors become progressively more ice-rich with time, or else the parent body accreted sufficiently far from the Sun that near-cosmic proportions of ice were condensed.

All of the scenarios considered here assume that carbonaceous chondrite parent bodies accreted at asteroidal distances with ice proportions of a few tens of percent. Alternatively, the original parent objects could have resembled comets, and later evolved into asteroid-like bodies (Wasson and Wetherill 1979). Aqueous alteration and oxygen-isotope exchange could occur during water-silicate differentiation (Grimm and McSween 1988), although an improved model might consider sinking of silicate grains through mobilized or partially melted ice. The mechanism for induration of cometary residues into lithified carbonaceous chondrites remain an open question, however.

In spite of the relative detail of the preliminary models developed here, further improvements are necessary to satisfy the observational constraints provided by carbonaceous chondrites. Explicit calculation of oxygen isotope exchange is needed to assess the total water volume present and the magnitude of variations in oxygen isotope abundance within the parent body. Better information on the rate-limiting processes for aqueous alteration is required— although alteration *can* occur rapidly, it may not always do so in nature. These ef-

forts would lead to time-dependent modeling of aqueous alteration. On a more fundamental level, criteria are needed to distinguish the formation location (inner or outer solar system), alteration environment (regolith or interior), and lithification mechanism of carbonaceous chondrites. Accretion processes and heat sources are also incompletely resolved.

The following conclusions can be drawn from this study:

(1) Mixtures of anhydrous silicates and ice are suitable starting compositions for carbonaceous chondrite parent bodies that have experienced aqueous alteration.

(2) Aqueous alteration may have occurred within either asteroidal interiors or surficial regoliths. Chemical, textural, and mechanical arguments support a petrologically homogeneous interior for the interior-alteration model and a large parent body for the regolith-alteration model.

(3) The fusion heat of ice, the high heat capacity of water, and the ability of circulating water to enhance rates of heat loss may all significantly contribute to thermal buffering of primordial heat sources for carbonaceous chondrite parent bodies.

(4) The short duration of both plausible primordial heat sources and relevant chemical reactions easily allows aqueous alteration to occur within time constraints imposed by radionuclide chronometers. In fact, exothermic hydration reactions probably require that water be gradually introduced into reaction sites to maintain low temperatures. Because the reverse reaction is endothermic, it is a thermal barrier, which may explain why little dehydration is observed in carbonaceous chondrites.

(5) For the interior-alteration model, bounds on initial $^{26}Al/^{27}Al$ ratios for CI chondrites are found comparable to those inferred or observed for both CO and ordinary chondrites. Model CI objects must be greater than several tens of kilometers in diameter to satisfy the interior homogeneity condition. CM chondrites require lower $^{26}Al/^{27}Al$ ratios, and model objects of this group do not develop the hydrothermal circulation that is probably necessary to satisfy water:rock ratios implied by oxygen isotope data.

(6) Regolith alteration may be driven by impacts or by internally generated heat sources. In internally heated models, temperatures at depth may reach levels higher than those allowed for interior-alteration models. Large quantities of water may be supplied to the regolith from below by hydrothermal circulation, vapor diffusion, or venting. Impacts can provide sufficient heat after parent bodies have accreted but may face difficulty in both delivering and maintaining required water volumes under alteration conditions.

(7) Retention of primordial ice in carbonaceous chondrite parent bodies is probably not limited by sublimation rates or by collisional comminution, but by shock vaporization.

(8) The present models cannot quantitatively account for all observational constraints imposed by different carbonaceous chondrite groups.

APPENDIX A: MATHEMATICAL FORMULATION OF THE CARBONACEOUS CHONDRITE THERMAL MODEL

The mathematical and numerical details are given here of the model used to calculate the internal evolution of carbonaceous chondrite parent objects. The principal assumptions adopted to arrive at this model are described in the text; only supporting details are given below. A summary of nomenclature is given at the end of this appendix, and all units are MKS unless noted otherwise.

Heat Flow

The spherically symmetric heat-conduction equation with internal heating,

$$\frac{\partial T}{\partial t} = \frac{1}{r^2} \frac{\partial}{\partial r} \left(r^2 \kappa \frac{\partial T}{\partial r} \right) + \frac{Q}{\rho c_p}, \quad \text{(A1)}$$

is solved by an implicit finite-difference method. The quantities in Eq. (A1) are tem-

perature T, radius r, thermal diffusivity κ, density ρ, specific heat c_p, and heat production per unit mass Q. The thermal conductivity is given by $k = \rho c_p \kappa$. The parameters that control thermal diffusion (k, ρ, and c_p) are taken as simple weighted sums of the contributions of rock, gas, and ice or water. The natural weights for k and ρ are relative volume, whereas the relative mass contributions govern c_p,

$$k = \frac{\sum_j k_j v_j}{\sum_j v_j}, \quad \rho = \frac{\sum_j \rho_j v_j}{\sum_j v_j},$$

$$c_p = \frac{\sum_j c_{p_j} m_j}{\sum_j m_j}, \quad (A2)$$

where v_j and m_j are the volume and mass fractions, respectively, of the jth component. From Eqs. (A2) it follows that

$$\kappa = \frac{\sum_j k_j v_j}{\sum_j \rho_j c_{p_j} v_j} \quad (A3)$$

for the effective thermal diffusivity. More precise formulations of effective thermal conductivity in two-phase media exist, such as the Maxwell formula (Carslaw and Jaeger, 1947), but the differences between (A2) and these formulations are minor for the present purpose. Temperature-dependent formulas for the thermodynamic and transport properties of rock and H_2O are given in a later section in this appendix.

The heat production Q is the sum of the heat production of individual radioactive elements, weighted by their time-dependent mean abundances in carbonaceous chondrites;

$$Q = m_r \sum_j A_{0j} Q_{0j} e^{-\lambda_j t}, \quad (A4)$$

where A_{0j} is the initial abundance, Q_{0j} is the initial heat production per unit mass, and λ_j is the decay constant of the jth radionuclide, and t is time. Since H_2O is also present, an overall weighting factor m_r, the mass fraction of rock, is required. The abundance of ^{26}Al, the primary heat-producing element in

TABLE A1

Assumed Abundances of Heat-Producing Elements

Nuclide	Initial abundance[a] (mass fraction)	Decay constant (year^{-1})	Initial heat production (W/kg)
^{26}Al	($^{26}Al/^{27}Al$) specified	9.63×10^{-7}	4.21×10^{3} ($^{26}Al/^{27}Al$)[b]
^{238}U	2.64×10^{-8}	1.55×10^{-10}	2.48×10^{-12}
^{235}U	8.60×10^{-9}	7.91×10^{-9}	4.98×10^{-12}
^{232}Th	5.21×10^{-8}	4.99×10^{-11}	1.36×10^{-12}
^{40}K	6.60×10^{-7}	5.48×10^{-10}	19.9×10^{-12}

[a] Observed C2 abundances (Mason 1971) extrapolated to $t = 4.60$ by before present.

[b] Using observed ^{27}Al abundance of 1.17 wt% in CM chondrites (Dodd 1981).

the model, is computed from the product of the assumed initial $^{26}Al/^{27}Al$ ratio and the observed mean Al content of CM chondrites. The relevant elemental abundances are given in Table A1.

The surface temperature is specified by solving the energy-balance equation

$$\frac{S_0}{4d^2}(1 - \mathscr{A}) = \varepsilon\sigma T^4 + k\left.\frac{\partial T}{\partial r}\right|_{r=R}, \quad (A5)$$

where S_0 is the solar constant, d is the orbital semimajor axis, $\mathscr{A}$ is the albedo, ε is the emissivity, σ is the Stefan–Boltzmann constant, and R is the object's radius. The loss of vapor is assumed to occur slowly, and its latent heat is neglected in (A5). This assumption follows from consideration of the characteristic time scale for surface degassing (Appendix B) and has been verified by numerical experiments.

Ice–Water Phase Transition

Melting of ice is assumed to occur at a temperature of 273°K, independent of pressure. Since lithostatic pressures exceed a kilobar only for the largest asteroids, the error in this approximation is generally less than 10°K. During the phase transition, thermal energy is absorbed as the latent heat of fusion,

$$\Delta T = \frac{M_i L_f}{M c_p}, \qquad \text{(A6)}$$

where ΔT is the temperature rise suppressed during melting, L_f is the latent heat of fusion of ice, and M and M_i are the total mass and mass of ice, respectively. Upon freezing, ΔT is the suppressed decrease in temperature. Temperature changes in regions of the phase transition are tracked using the algorithm of Reynolds et al. (1966), which uses a partial melt state and associated partial release and absorption of fusion heat to avoid numerical instabilities associated with finite time steps.

Hydrothermal Convection

Closed circulation of heated water may occur within the asteroid under favorable conditions and provide significant heat transfer. A simple parameterized convection scheme is adopted, similar to calculations of the thermal histories of the Earth (Sharpe and Peltier 1978), the Moon and the terrestrial planets (Cassen et al. 1979, Schubert et al. 1979, Turcotte et al. 1979), and the Galilean satellites (Thurber et al. 1980).

Buoyant instability in a porous layer of thickness r_w heated from below, with permeability K and average thermal conductivity k, occurs when the Rayleigh number

$$Ra = \frac{\rho_w^2 g \alpha_w c_{p_w} K \Delta T r_w}{\eta_w k} \qquad \text{(A7)}$$

exceeds the critical value $Ra_{cr} = 4\pi^2 \cong 39$ (e.g., Turcotte and Schubert 1982), where ρ_w is the reference density of water, g is the gravitational acceleration, α_w is the thermal expansion coefficient of water, ΔT is the temperature drop across the layer, and η_w is the viscosity of water. The efficiency of convection is measured by the Nusselt number Nu, which is the ratio of the total heat transported out of the convecting layer to the heat transported by conduction alone, $Nu = q/q_c$. The relation between Ra and Nu has been numerically investigated for two dimensional hydrothermal convec-

tion by Straus (1974). These results are approximately described by the empirical formulas

$$\begin{aligned} Nu &= Ra'^{1.3}, \qquad Ra' < 2, \\ Nu &= 1.6\, Ra'^{0.6}, \quad Ra' > 2, \end{aligned} \qquad \text{(A8)}$$

where $Ra' = Ra/Ra_{cr}$. When the layer is heated from within instead of from below, the reciprocal of the nondimensional temperature difference across the layer measures steady-state convective efficiency (Turcotte et al. 1979); however, Nu may be used for the transient problem when the heat production per time step is small (Cassen et al. 1979).

In the parameterized convection approach, an equivalent conductive solution is sought that has the same heat transfer as the convective system; this may be accomplished by solving (A1) with an effective thermal diffisivity $Nu\,\kappa$ (Sharpe and Peltier 1978). Since the model is spherically symmetric, this thermal profile represents an azimuthal average of the convective temperature field's hot upwellings and cool downwellings. The "actual" azimuthally averaged temperatures are not those of the equivalent conductive solution, however, but must follow an adiabat within the convecting region. Since the slope of the H_2O adiabat is small at the low gravitational accelerations relevant to this problem, the circulating region is approximately isothermal: its temperature is calculated by matching the total thermal energy from the equivalent conductive solution (Cassen et al. 1979). A boundary layer of thickness $\sim r_w/Nu$ exists at the top of the convecting layer and is neglected in computing "actual" temperature profiles; this approximation is valid for $Nu \gg 1$.

Since convection is not limited to upper layers in the object, the effects of spherical geometry will strongly influence the growth of density perturbations and the resulting flow. An analysis of the stability of an internally heated porous sphere has not been found in the literature. However, comparison of the conditions of the onset of con-

vection (Chandresekhar 1961) for an internally heated fluid sphere and for a fluid layer heated from below (with mean gravitational acceleration of the sphere) shows that, for the same temperature drop, convection in the sphere requires Ra' approximately twice as large as that for the layer. The initiation of instability in the sphere is inhibited by the smaller buoyancy forces resulting from decreased relative volume and lower gravity in the deep interior. Furthermore, Turcotte *et al.* (1979) showed that steady-state heat transfer is more efficient for the layer than for the sphere at the same value of Ra'. Use of (A7)–(A8), therefore, must also yield an overestimate of the convective efficiency of the porous sphere. The error is conservative, however, because an upper limit on the efficiency of heat transfer must be used to constrain upper bounds on the size and heat production of carbonaceous chondrite parent objects. The layer approximation satisfies this constraint and renders the problem tractable.

A further limitation to the parameterized convection approach is that the stability analysis which leads to the derivation of Ra requires that all properties be constant, with the exception of a linear temperature-dependent variation of density (Boussinesq approximation). Such an approximation is not always satisfied in hydrothermal systems with temperature variations of several hundred degrees; density variations are of order unity, and viscosity variations may span an order of magnitude. Terrestrial hydrothermal convection in a medium of variable thermodynamic properties was studied by Straus and Schubert (1977), who found that Ra_{cr} may be much smaller than the Boussinesq value ($\sim$39). These results may be applied to asteroidal interiors by noting from (A7) that the thickness of a layer for which instability occurs scales inversely with gravity. Employing the scaled layer thickness and full temperature interval over which H_2O is liquid, we find from the work of Straus and Schubert that Ra_{cr} may be significantly reduced for objects with diameters greater than 300 km. By using volume-averaged properties in (A7), some of these effects may be suppressed; nevertheless, this nonlinearity remains a potential source of error since it does not lead to upper limits to heat production.

Hydrothermal convection will be limited by the degree of H_2O saturation of the pore volume. If water does not completely fill the pores, the medium may be treated as one of reduced effective permeability. The effective porosity in the unsaturated state is just the water volume fraction v_w, and, if the Kozeny–Carman relation (e.g., Lambe and Whitman 1969) is used, the effective permeability may be expressed as

$$K = K_0 \frac{e/(1 + e)}{e_0/(1 + e_0)}, \qquad (A9)$$

where e is the void ratio ($e = \phi/(1 - \phi)$, where ϕ is the porosity) and the zero subscript denotes the saturated state. Since the variation in K_0 between different rock types spans several orders of magnitude, the onset of convection (and the rate of H_2O vapor loss, discussed below) is very sensitive to the permeability. Arguments for the choices of this parameter are discussed in the text.

The key assumption in evaluating effective permeability in unsaturated states is that water remains continuously interconnected within the pores. In soil mechanics, the maximum capillary head defines the height over which water remains in contact following draining of a soil (Lambe and Whitman 1969). Since capillary head is inversely proportional to both gravity and pore dimension (Batchelor 1967), very large capillary zones, in the range 1–1000 km for pore dimensions of 1 μm to 1 mm, may exist in carbonaceous chondrite parent objects ($g \sim 10^{-2}$ m sec^{-2}). Even if water were not continuously interconnected, it is conservative to assume so, for reasons given previously, in order to provide favorable conditions for convective heat transfer.

Gas Diffusion

The principal assumption of the vapor transport model is that the interior is in a state of quasi-static equilibrium. Under these conditions, the gas pressure always adjusts rapidly to the local temperature and H_2O volume, which change in response to diffusion of gas and thermal energy.

From the Clausius–Clapeyron relation, the vapor pressure has the approximate form

$$P_{vap} = P_0 e^{-T_0/T}, \qquad (A10)$$

where P_0 and T_0 have dimensions of pressure and temperature, respectively. By fitting data given in Keyes (1928) and Washburn (1928), we adopt $P_0 = 3.58 \times 10^{12}$ Pa, $T_0 = 6140°K$ for the vapor pressure over ice, and $P_0 = 4.70 \times 10^{10}$ Pa, $T_0 = 4960°K$ for the vapor pressure over water.

The equation of state used for H_2O vapor or gas is

$$PV = n\Re T \quad (T < 500°K),$$

$$\left(P + \frac{n^2 a}{V^2}\right)(V - nb) = n\Re T \quad (T > 500°K), \qquad (A11)$$

where P is the ambient vapor or gas pressure, V is volume, n is the number of moles of H_2O, $\Re$ is the universal gas constant, and a and b are the van der Waals coefficients. From (A11) the gas density $\rho_g = n\mathcal{M}/V$ may be found ($\mathcal{M}$ is the molar mass); vapor–condensate mass balance then yields the mass of gas M_g in a specified volume of the asteroidal interior,

$$M_g = \rho_g V_g = \frac{\rho_c V\phi - M_0}{\rho_c/\rho_g - 1}, \qquad (A12)$$

where V_g is the volume of gas, ρ_c is the density of condensate (ice or water), V is the total volume, ϕ is the porosity, and M_0 is the total mass of H_2O.

The diffusion of H_2O through the interior must satisfy the equation of continuity

$$\frac{1}{r^2} \frac{\partial}{\partial r} (r^2 \rho u) = -\frac{\partial \rho}{\partial t} \qquad (A13)$$

and Darcy's law

$$u = -\frac{K}{\eta} \frac{\partial P}{\partial r}, \qquad (A14)$$

where u is the vertical velocity, η is the viscosity, K is the permeability, and gravitational forces, which are small, have been neglected. Equations (A13) and (A14) may be combined into the nonlinear equation

$$\frac{\partial \rho}{\partial t} = \frac{1}{r^2} \frac{\partial}{\partial r} \left(r^2 \frac{K\rho}{\eta} \frac{\partial P}{\partial r}\right), \qquad (A15)$$

which is solved by an explicit finite-difference method. The gas mass transferred in a given time step is $\Delta M_g = \Delta \rho_g V_g$. An advective temperature change

$$\Delta T = -\frac{\Delta M_g L_v}{M c_{pg}} \qquad (A16)$$

is caused by the net evaporation or condensation of vapor at a particular location, where L_v is the latent heat of vaporization. Equation (A16) holds only when condensate is present and the small change associated with the product of the gas's heat capacity c_{pg} and the temperature difference between adjacent grid locations is neglected.

In this treatment of the gas diffusion problem, H_2O gas and condensate are considered immiscible fluids. The permeability is calculated from (A9), using v_g for the effective porosity and $1 - v_r$ for the reference porosity. At low temperatures, however, the efficiency of diffusion may be greatly enhanced by free molecular (Knudsen) flow, which occurs when the mean free path of a gas molecule is significantly larger than the characteristic pore dimension,

$$\frac{\Re T}{4\sqrt{2}\pi N_A P_{vap} b^2} \gg d, \qquad (A17)$$

where N_A is Avogadro's number, b is the radius of the H_2O molecule, and d is the pore size. Equation (A17) may be solved as an equality for the approximate transition temperature to Knudsen flow under equilibrium conditions. Following Sugiura et al.

(1984), one may parameterize free molecular flow as an increase in the effective permeability inversely proportional to the vapor pressure at temperatures below the transition temperature. In practice, Knudsen flow is of little importance during the active thermal history of the asteroid but becomes relevant to the treatment of secular degassing (Appendix B).

Venting of H_2O

Gas diffusion obeying (A14) will generally be smooth, unless pressures become so large that failure occurs. In this case H_2O may move rapidly to upper levels in the asteroid where it may recondense in available pores or escape directly into space. Failure occurs when the pore pressure exceeds the sum of the lithostatic pressure and the tensile strength of the rock (Jaeger and Cook 1976):

$$P > P_{lith} + \tau. \qquad (A18)$$

The lithostatic pressure is given by

$$P_{lith} = \frac{4}{3} \pi G \int_0^R \rho_r^2 r \, dr. \qquad (A19)$$

When gas fracturing occurs, H_2O has a direct path to the surface and might be free to boil away completely in an isothermal environment. However, advective heat losses will limit the rate of venting. In practice, (A16) is solved for the vented gas mass due to a temperature increase in a given time step, and the temperature is then reset to its original value, so that heating at a given location is balanced by venting of gas. As long as condensate is available, the temperature is constant and the pressure is maintained at the failure strength. The vented H_2O may be expressed as the thickness of a saturated surface layer of equal volume as a convenient measure of the depth to which significant liquid water may be available in the regolith.

An additional failure mode, hydraulic fracturing, is possible when thermal expansion would lead to a volume of water in excess of the available pore volume. In this case, the pressure is given by

$$P = B \left(\frac{V_w - \phi V}{\phi V} \right), \qquad (A20)$$

where B is the bulk modulus of water, ϕV is the total pore volume, and V_w is the volume to which water would expand. If (A18) is satisfied, the difference between these volumes is lost by hydraulic fracturing.

Hydration and Dehydration Reactions

The formation of serpentine and brucite from forsterite and water is taken to represent the reactions characterizing aqueous alteration of carbonaceous chondrites:

$$2 \, Mg_2SiO_4 + 3 \, H_2O = Mg_3Si_2O_5(OH)_2$$
$$+ \, Mg(OH)_2. \qquad (A21)$$
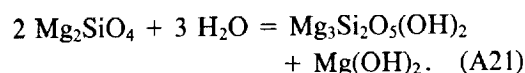
The water:rock volume ratio of the reactants, which is denoted β, is 0.63, and the volume ratio of the products to the reacting forsterite, which is denoted γ, is 1.56. Assuming that net volume changes between the silicate phases are accommodated entirely by the pore volume, i.e., there is no net expansion of the asteroid, the volume balance for (A21) is

$$\Delta v_a + \Delta v_h + \Delta v_w + \Delta v_v = 0,$$
$$\Delta v_w / \Delta v_a = \beta, \quad \Delta v_h / \Delta v_a = -\gamma, \qquad (A22)$$

where Δv is the change in volume fraction and the subscripts a, h, w, and v imply anhydrous minerals (forsterite), hydrous minerals (serpentine and brucite), water, and voids, respectively. Note that $\phi = v_w + v_v$. For the hydration (retrograde) reaction, two cases may be distinguished. If $v_w / \beta < v_a$, then incomplete alteration of anhydrous minerals will occur, and all water will be exhausted. If $v_w / \beta > v_a$, then complete alteration of all anhydrous minerals occurs, and some excess water remains. Using only the subscripts, the changes in volume fraction for incomplete hydration are

$$\Delta w = -w, \quad \Delta a = -w/\beta, \quad \Delta h = \gamma w/\beta,$$
$$\Delta v = -w(1 + \beta - \gamma)/\beta \qquad (A23)$$

and the fractional volume changes for complete hydration are

$$\Delta a = -a, \quad \Delta w = -\beta a, \quad \Delta h = \gamma a,$$
$$\Delta v = -a(\gamma - \beta - 1). \quad (A24)$$

From the standard heats of formation tabulated by Robie and Waldbaum (1968), the heat of reaction released at 25°C is $H = 233$ kJ/kg. The increase in temperature is

$$\Delta T = \frac{\Delta M_h H}{M c_p}, \quad (A25)$$

where ΔM_h is the mass of hydrous minerals formed by the reaction. Since the reaction time is small compared with the thermal diffusion time (see text), formation of hydrous minerals and release of reaction heat are assumed to occur instantaneously upon complete melting of ice.

The equilibrium phase boundary for this reaction has been determined by Johannes (1968) to lie at ~360°C at a fluid pressure of 1 kbar. Fluid pressures in asteroids will usually lie below this value, even if they approach lithostatic pressure. Therefore, 350°C is taken to be the temperature of the dehydration (prograde) reaction. All hydrous minerals are assumed to dehydrate instantaneously, resulting in the fractional volume changes

$$\Delta h = -h, \quad \Delta a = h/\gamma, \quad \Delta w = \beta h/\gamma,$$
$$\Delta v = h(\gamma - \beta - 1)/\gamma. \quad (A26)$$

The changes in the enthalpies of forsterite and brucite at 600°K are negligible, and the enthalpy of water changes by only 14%. The high-temperature enthalpy of serpentine was not given by Robie and Waldbaum (1968), but changes in other phyllosilicate minerals are also negligible. The heat of the dehydration reaction at 350°C, then, is assumed to be -233 kJ/kg. When the temperature falls below 350°C, rehydration of the silicates occurs. In practice, temperature changes are evaluated by the algorithm that is used for melting and freezing of ice, by using a partial reaction state to avoid numerical instabilities.

Temperature-Dependent Material Properties

The low-temperature thermal diffusivity of rock is taken to be that measured by Yomogida and Matsui (1983) for Leoville (CV3):

$$\kappa_r = 3.02 \times 10^{-7} + 2.78 \times 10^{-4}/T.$$

Since the mineralogies of unaltered and altered rock are considered to be roughly those of olivine and serpentine, the density of rock ρ_r is taken to be either 3.3 or 2.5 Mg/m^3, respectively. Specific heat measurements of carbonaceous chondrites are lacking, so c_{pr} is taken to be 700 J/kg-°K, a typical value for ordinary chondrites (Alexeyeva 1958, Yomogida and Matsui 1983).

Since 400°K was the highest temperature at which measurements on Leoville were performed by Yomogida and Matsui (1983), k_r is dominated by lattice phonon conductivity. At higher temperatures, radiation becomes important. On the basis of thermal measurements of olivine and pyroxene, Schatz and Simmons (1972) include a radiative conductivity term that is directly proportional to temperature above 500°K. Assuming that the total thermal conductivity between 500 and 1000°K of the minerals measured by Schatz and Simmons (1972) and that of Leoville differ by a multiplicative constant, the total (lattice + radiative) conductivity k_r' is

$$k_r' = k_r + 2.1 \times 10^{-3} (T - 500°K)$$

at temperatures greater than 500°K.

The thermal conductivity and heat capacity of hexagonal ice are given by Hobbs (1974),

$$k_i = 0.465 + 488/T,$$

$$c_{pi} = 7.67 \, T,$$

and, for simplicity, the density of ice is taken to be $\rho_i = 1.0$ Mg/m^3. Since amorphous ice is unstable at $T > 135°K$ (Klinger 1980), its different thermal properties need not be considered at temperatures typical of asteroidal surfaces.

A forth-order polynomial was constructed for the density of water, by fitting measurements summarized by Keyes (1928):

$$\rho_w = -221 + 13.1\,T - 5.07 \times 10^{-2}\,T^2 + 8.49 \times 10^{-5}\,T^3 - 5.48 \times 10^{-8}\,T^4.$$

Gaseous H_2O is taken to behave ideally below 500°K and as a van der Waals gas at higher temperatures; the density ρ_g may be calculated from the relevant equation of state. Details are given above in the section on gas diffusion.

The thermal conductivity of H_2O liquid and gas are given by Touloukian et al. (1970):

$$k_w = -0.581 + 6.34 \times 10^{-3}\,T - 7.93 \times 10^{-6}\,T^2, \quad T < 410°K,$$

$$k_w = -0.142 + 4.12 \times 10^{-3}\,T - 5.01 \times 10^{-6}\,T^2, \quad T > 410°K,$$

$$k_g = -1.43 \times 10^{-2} + 1.02 \times 10^{-4}\,T.$$

The specific heat of water is given by Touloukian and Makita (1970), and the specific heat of gaseous H_2O was taken from Zemansky and Dittman (1981),

$$c_{pw} = 4200, \quad T < 410°K,$$

$$c_{pw} = -4.67 \times 10^4 + 333\,T - 0.731 \, T^2 + 5.40 \times 10^{-4}\,T^3 \quad T > 410°K,$$

$$c_{pg} = 1680 + 0.552\,T,$$

where the small variation in the specific heat of water below 400°K and higher-order terms in the specific heat H_2O gas have been neglected.

The viscosity of H_2O liquid and gas is given by Touloukian et al. (1975):

$$\eta_w = 2.414 \times 10^{-5} \, 10^{247.8/(T-140)},$$

$$\eta_g = 8.04 \times 10^{-6} + 4.07 \times 10^{-8}\,T.$$

Nomenclature

a first van der Waals coefficient for H_2O, 0.546 m^6 mole^{-2}

a   (subscript) anhydrous rock

A radioactive element abundance, wt fraction

$\mathscr{A}$ albedo

b second van der Waals coefficient for H_2O, 3.05 $\times$ 10^{-5} m^3 mole^{-1}

b radius of water molecule, ~5 $\times$ 10^{-11} m

B bulk modulus of water, 2 $\times$ 10^9 Pa

c   (subscript) H_2O condensate (water or ice)

c_p specific heat capacity at constant pressure, J kg^{-1} °K^{-1}

d orbital semimajor axis, m

d grain or pore diameter, m

D object diameter, m

e void ratio

g gravitational acceleration, m sec^{-2}

g   (subscript) gas

G gravitational constant, 6.67 $\times$ 10^{-11} N m^2 kg^{-2}

h   (subscript) hydrated rock

H heat of reaction for 2 Fo + 3 H_2O = serp + bru, 2.33 $\times$ 10^5 J kg^{-1}

i   (subscript) ice

j summation index for bulk rock–H_2O composition or radionuclides

k thermal conductivity, W/m-°K

K permeability, m^2

K_0 reference permeability, m^2

L_f latent heat of fusion of H_2O, 3.34 $\times$ 10^5 J kg^{-1}

L_v latent heat of vaporization of H_2O, 2.26 $\times$ 10^6 J kg^{-1}

m mass fraction

M mass, kg

$\mathcal{M}$ molar mass of H_2O, 18 $\times$ 10^{-3} kg mole^{-1}

n moles

N_A Avogadro's number, 6.02 $\times$ 10^{23} molecules mole^{-1}

Nu Nusselt number

P pressure, Pa

P_0 pressure parameter for vapor pressure equation

Q radionuclide heat generation, W kg^{-1}

r radius, m

r   (subscript) rock

r_w radius of liquid water, i.e., width of potential convecting layer

R object radius, m

$\mathscr{R}$ universal gas constant, 8.314 J mole^{-1} °K^{-1}

Ra Rayleigh number

Ra' Rayleigh number, expressed as multiple of critical value

S_0 solar constant, 1360 W m^{-2}

t time, sec

T temperature, °K

T_0 temperature parameter for vapor pressure equation

u velocity, m/sec

v volume fraction

v   (subscript) void

V volume, m^3

α volumetric coefficient of thermal expansion, °K^{-1}

β water/rock volume fraction for hydration

γ volume expansion factor of hydrous minerals

ε emissivity

η viscosity, Pa-sec

κ thermal diffusivity, m^2 sec^{-1}

λ radionuclide decay constant, sec^{-1}

ρ density, kg/m^3

σ Stefan–Boltzmann constant, 5.67 × 10^{-8} W m^{-2} °K^{-4}

τ tensile strength, Pa

ϕ porosity

APPENDIX B: DEGASSING AND SECULAR RETENTION OF H₂O

The model derived in Appendix A may be used to calculate the diffusion of H₂O throughout an asteroidal interior and the eventual loss of volatiles to space. In this appendix, a simple dimensional analysis of the degassing from the asteroidal surface is given, and a relation is derived for the depth to which free H₂O should be largely depleted as a function of orbital semimajor axis and regolith permeability.

Consider the one-dimensional diffusion of a constant-viscosity gas at low temperature in a medium of fixed permeability. Gas transport must satisfy the equation of state, the continuity equation, and Darcy's law,

$$PV = n\Re T,$$

$$\frac{\partial(\rho u)}{\partial z} = -\frac{\partial \rho}{\partial t}, \quad u = -\frac{K}{\eta}\frac{\partial P}{\partial z}, \quad \text{(B1)}$$

where all symbols follow the definitions given in Appendix A. Equations (B1) may be combined into the single equation

$$\frac{\partial P}{\partial t} = \frac{K}{\eta}\left[P\frac{\partial^2 P}{\partial z^2} + \left(\frac{\partial P}{\partial z}\right)^2\right]. \quad \text{(B2)}$$

Dimensional analysis of (B2) gives, to order of magnitude,

$$\frac{\Delta P}{\Delta t} = \frac{K}{\eta}\frac{\Delta P^2}{\Delta z^2}, \quad \text{(B3)}$$

from which follows the time scale t_0 for degassing,

$$t_0 = \frac{\eta \Delta z^2}{K \Delta P}. \quad \text{(B4)}$$

Equation (B4) applies to a region without gas sources. However, if the interior is in a state of vapor–condensate equilibrium, a special, self-limiting source exists: the vapor pressure P_{vap} is maintained as long as condensate is available. Under equilibrium conditions, the amount of vapor, expressed in moles, is just $n_{vap} = v_v P_{vap} V/\Re T$, where v_v is the volume fraction of voids ($\sim 1 - v_r - v_i$). Since asteroidal interiors are nearly isothermal over most of solar system history, the vapor pressure may be evaluated at the surface temperature, and the pressure drop from the surface through the degassed zone to the region of vapor–condensate equilibrium is $\Delta P = P_{vap}$. From (B4), then, an amount of H₂O $\sim n_{vap}$ is lost on a time scale t_0. However, the total amount of H₂O present is $n_{tot} = v_i \rho_i V/\mathcal{M}$, where $\mathcal{M}$ is the molar mass. Therefore the number of characteristic degassing time scales that can be endured before ice is exhausted is

$$N = n_{tot}/n_{vap} = v_i \rho_i \Re T/v_v \mathcal{M} P_{vap}. \quad \text{(B5)}$$

If the comparable quantities v_i and v_v are dropped, the *total* degassing time scale, $t = Nt_0$, is

$$t = \frac{\rho_i \eta \Re T \Delta z^2}{K \mathcal{M} P_{vap}^2}, \quad \text{(B6)}$$

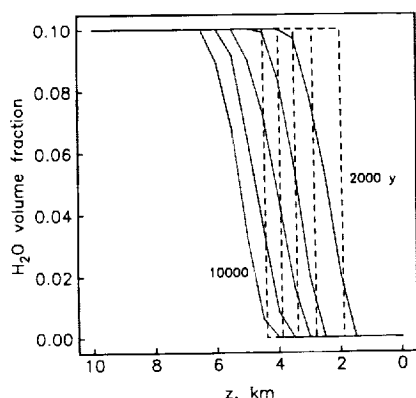which may be rearranged to give the depth scale Δz of degassing over time scale t:

FIG. B1. Example of one-dimensional vapor diffusion at 1-AU solar distance, for a regolith with 10% H_2O volume, 25% porosity, and permeability 10^{-7} m^2. Numerical calculation (solid curves) compares well with simple approximation (dashed curves) from dimensional analysis for the depth of nearly complete H_2O loss.

$$\Delta z = P_{vap}(T) \sqrt{\frac{K\mathcal{M}t}{\rho_i \eta \mathfrak{R} T}}. \qquad (B7)$$

Substituting (A10) for the vapor pressure and (A5) for the surface temperature, one may find Δz as a function of permeability and orbital semimajor axis. Figure B1 compares the approximate result (B7) with a numerical calculation performed using the analysis given in Appendix A, with $K = 10^{-7}$ m^2, $\eta = 10^{-5}$ Pa-sec, and at a distance of 1 AU. Reasonable agreement is found for the depth of the devolatized zone as a function of time. In contrast, the time scales for similar degassing depths given by (B4) or by the rate of free sublimation (e.g., Zemansky and Dittman 1981) are only a month or less.

ACKNOWLEDGMENTS

REFERENCES

AKAI, J. 1988. Incompletely transformed serpentine-type phyllosilicates in the matrix of Antarctic meteorites. *Geochim. Cosmochim. Acta* **52**, 1593–1599.

ALEXEYEVA, K. N. 1958. Physical properties of stony meteorites and their interpretation in the light of hypotheses regarding the origin of the meteorites. *Meteoritika* **17**, 67–77. [in Russian]

ANDERS, E., AND M. EBIHARA 1982. Solar-system abundances of the elements. *Geochim. Cosmochim. Acta* **44**, 1543–1577.

BARBER, D. J. 1981. Matrix phyllosilicates and associated minerals in C2M carbonaceous chondrites. *Geochim. Cosmochim. Acta* **45**, 945–970.

Basaltic Volcanism Study Project 1981. *Basaltic Volcanism on the Terrestrial Planets.* Pergamon, New York.

BATCHELOR, G. K. 1967. *An Introduction to Fluid Dynamics.* Cambridge Univ. Press, Cambridge.

BELL, J. P. 1986. Mineralogical evolution of meteorite parent bodies (abstract). In *Lunar and Planetary Science XVII*, pp. 985–986. Lunar and Planetary Institute, Houston, TX.

BRATT, S. R., S. C. SOLOMON, AND J. W. HEAD 1985. The evolution of impact basins: Cooling, subsidence, and thermal stress. *J. Geophys. Res.* **90**, 12415–12433.

BUDDHUE, J. D. 1942. The compressive strength of meteorites. *Contrib. Soc. Res. Meteorites* **3**, 39–40.

BUNCH, T. E., AND S. CHANG 1980. Carbonaceous chondrites. II. Carbonaceous chondrite phyllosilicates and light element geochemistry as indicators of parent body processes and surface conditions. *Geochim. Cosmochim. Acta* **44**, 1543–1577.

CAFFEE, M. W., AND J. D. MACDOUGALL 1988. Compaction ages. In *Meteorites and the Early Solar System* (J. F. Kerridge and M. S. Matthews, Eds.), pp. 289–298. Univ. of Arizona Press, Tucson.

CAIN, P. M., H. Y. McSWEEN, JR., AND N. B. WOODWARD 1986. Structural deformation of the Leoville chondrite. *Earth Planet. Sci. Lett.* **77**, 165–175.

CAMERON, A. G. W., AND M. R. PINE 1973. Numerical models of the primitive solar nebula. *Icarus* **18**, 377–406.

CARSLAW, H. S., AND J. C. JAEGER 1947. *Conduction of Heat in Solids.* Oxford Univ. Press, London.

CASSEN, P., R. T. REYNOLDS, F. GRAZIANI, A. SUMMERS, J. McNELLIS, AND L. BLALOCK 1979. Convection and lunar thermal history. *Phys. Earth. Planet. Int.* **19**, 183–196.

CHANDRASEKHAR, S. 1961. *Hydrodynamic and Hydromagnetic Stability.* Oxford University Press, London.

CHAPMAN C. R., AND W. B. McKINNON 1986. Cratering of planetary satellites. In *Satellites* (J. A. Burns and M. S. Matthews, Eds.), pp 492–580. Univ. of Arizona Press, Tucson.

CLAYTON, R. N., AND T. K. MAYEDA 1984. The oxygen isotope record in Murchison and other carbonaceous chondrites. *Earth Planet. Sci. Lett.* **67**, 151–161.

COSTES, N. C., AND J. K. MITCHELL 1970. Apollo 11 soil mechanics investigation. *Proc. Apollo 11 Lunar Sci. Conf., Geochim. Cosmochim. Acta., Suppl.,* 2025–2044.

DAVIS, D. R., C. R. CHAPMAN, R. GREENBERG, S. WEIDENSCHILLING, AND A. W. HARRIS 1979. Collisional evolution of asteroids: Populations, rotations, and velocities. In *Asteroids* (T. Gehrels, Ed.), pp. 528–557. Univ. of Arizona Press, Tuscon.

DODD, R. T. 1981. *Meteorites: A Petrologic-Chemical Synthesis.* Cambridge Univ. Press, Cambridge.

DODD, R. T., AND E. JAROSEWICH 1979. Incipient melting in and shock classification of L-group chondrites. *Earth Planet. Sci. Lett.* **44**, 335–340.

DOMINIK, B., AND E. K. JESSBERGER 1979. ^{40}Ar–^{39}Ar dating of Murchison, Allende, and Leoville whole rock samples (abstract). In *Lunar and Planetary Science X,* pp. 306–308. Lunar and Planetary Institute, Houston, TX.

DuFRESNE, E. R., AND E. ANDERS 1962. On the chemical evolution of the carbonaceous chondrites. *Geochim. Cosmochim. Acta* **26**, 1085–1114.

FREDRIKSSON, K., AND J. F. KERRIDGE 1988. Carbonates and sulfates in CI chondrites: Formation by aqueous activity on the parent body. *Meteoritics* **23**, 35–44.

GOETTEL, K. A., AND S. S. BARSHAY 1978. The chemical equilibrium model for condensation in the solar nebula: Assumptions, implications, and limitations. In *The Origin of the Solar System* (S. F. Dermott, Ed.), pp. 611–627. Wiley, New York.

GOSWAMI, J. N., D. LAL, AND L. L. WILKENING 1984. Gas-rich meteorites: Probes for particle environment and dynamical processes in the inner solar system. *Space Sci. Rev.* **37**, 111–159.

GRADIE, J., AND E. TEDESCO 1982. Compositional structure of the asteroid belt. *Nature* **216**, 1405–1407.

GREENBERG, R., AND C. R. CHAPMAN 1983. Asteroids and meteorites: Parent bodies and delivered samples. *Icarus* **55**, 455–481.

GREENBERG, R., J. F. WACKER, W. K. HARTMANN, AND C. R. CHAPMAN 1978. Planetesimals to planets: Numerical simulation of collisional evolution. *Icarus* **35**, 1–26.

GRIMM, R. E. 1985. Penecontemporaneous metamorphism, fragmentation, and reassembly of ordinary chondrite parent bodies. *J. Geophys. Res.* **90**, 2022–2028.

GRIMM, R. E., AND H. Y. McSWEEN, JR. 1988. Water and the thermal history of the CM carbonaceous chondrite parent body (abstract). In *Lunar and Planetary Science XIX,* pp. 427–428. Lunar and Planetary Institute, Houston, TX.

GROSSMAN, L. 1972. Condensation in the primitive solar nebula. *Geochim. Cosmochim. Acta* **36**, 597–619.

HARTMANN, W. K. 1969. Terrestrial, lunar, and interplanetary rock fragmentation. *Icarus* **31**, 168–174.

HERBERT, F., AND C. P. SONETT 1979. Electromagnetic heating of minor planets in the early solar system. *Icarus* **48**, 484–496.

HOBBS, P. V. 1974. *Ice Physics.* Clarendon, Oxford.

HOUSEN, K. R., L. L. WILKENING, C. R. CHAPMAN, AND R. J. GREENBERG 1979. Asteroidal regoliths. *Icarus* **39**, 317–351.

HUTCHEON, I. D., R. HUTCHISON, AND G. J. WASSERBURG 1989. Evidence from the Semarkona ordinary chondrite for ^{26}Al heating of small planets. *Nature* **337**, 238–241.

JAEGER, J. C., AND N. G. W. COOK 1976. *Fundamentals of Rock Mechanics.* Chapman & Hall, London.

JOHANNES, W. 1968. Experimental investigation of the reaction forsterite + H_2O = serpentine + brucite. *Contrib. Mineral. Petrol.* **19**, 309–315.

JONES, T. D., L. A. LEBOFSKY, AND J. S. LEWIS 1988. The 3-μm hydrated silicate signature on C class asteroids: Implications for origins of outer belt objects (abstract). In *Lunar and Planetary Science XIX,* pp. 567–568. Lunar and Planetary Institute, Houston, TX.

KAULA, W. M. 1979. Thermal evolution of the Earth and Moon growing by planetesimal impacts. *J. Geophys. Res.* **84**, 999–1008.

KERRIDGE, J. F., AND T. E. BUNCH 1979. Aqueous activity on asteroids: Evidence from carbonaceous chondrites. In *Asteroids* (T. Gehrels, Ed.), pp. 745–764. Univ. of Arizona Press, Tucson.

KEYES, F. G. 1928. Vapor pressures and orthobaric volumes for H_2O, NH_3, CO_2, and SO_2 above one atmosphere. In *International Critical Tables,* Vol. 3 (E. W. Washburn, (Ed.), pp. 233–236, McGraw-Hill, New York.

KIEFFER, S. W., AND C. H. SIMONDS 1980. The role of volatiles and lithology in the impact cratering process. *Rev. Geophys. Space Phys.* **18**, 143–181.

KLINGER, J. 1980. Influence of a phase transition of ice on the heat and mass balance of comets. *Science* **209**, 271–272.

LAMBE, T. W., AND R. V. WHITMAN 1969. *Soil Mechanics.* Wiley, New York.

LANGE, M. A., P. LAMBERT, AND T. J. AHRENS 1985. Shock effects on hydrous minerals and implications for carbonaceous chondrites. *Geochim. Cosmochim. Acta* **49**, 1715–1726.

LEBOFSKY, L. A., M. A. FEIERBERG, A. T. TOKUNAGA, H. P. LARSON, AND J. R. JOHNSON 1981. The 1.7 to 4.2-mm spectrum of asteroid 1 Ceres: Evidence for structural water in clay minerals. *Icarus* **48**, 453–459.

LEE, T., D. A. PAPANASTASSIOU, AND G. J. WASSERBURG (1976). Correction: Demonstration of excess ^{26}Mg in Allende and evidence for ^{26}Al. *Geophys. Res. Lett.* **3**, 109–112.

LEWIS, J. S. 1972. Low-temperature condensation from the solar nebula. *Icarus* 16, 241–252.

MACDOUGALL, J. D., AND B. K. KOTHARI 1976. Formation chronology for C2 chondrites. *Earth Planet. Sci. Lett.* 33, 36–44.

MACDOUGALL, J. D., G. W., LUGMAIR, AND J. F. KERRIDGE 1984. Early solar system aqueous activity: Sr isotope evidence from the Orgueil CI meteorite. *Nature* 307, 249–251.

MACKINNON, I. D. R., AND M. ZOLENSKY 1984. Proposed structures of poorly characterized phases in C2M carbonaceous chondrite meteorites. *Nature* 309, 240–242.

MASON, B. 1971. *Handbook of Elemental Abundances in Meteorites*. Gordon & Breach, New York.

McSWEEN, H. Y., JR. 1977. Carbonaceous chondrites of the Ornans type: A metamorphic sequence. *Geochim. Cosmochim. Acta* 41, 477–491.

McSWEEN, H. Y., JR. 1979. Are carbonaceous chondrites primitive or processed? A review. *Rev. Geophys. Space Phys.* 17, 1059–1078.

McSWEEN, H. Y., JR. 1987. Aqueous alteration in carbonaceous chondrites: Mass balance constraints on matrix mineralogy. *Geochim. Cosmochim. Acta* 51, 2469–2477.

McSWEEN, H. Y., JR., AND S. M. RICHARDSON 1977. The composition of carbonaceous chondrite matrix. *Geochim. Cosmochim. Acta* 41, 1145–1161.

MERCER, J. W., G. F. PINDER, AND I. G. DONALDSON 1975. A Galerkin-finite element analysis of the hydrothermal system at Wairakei, New Zealand. *J. Geophys. Res.* 80, 2608–2621.

MITTLEFEHLDT, D. W., AND G. W. WETHERILL 1979. Rb-Sr studies of CI and CM chondrites. *Geochim. Cosmochim. Acta* 43, 201–206.

MIYAMOTO, M., N. FUJII, AND H. TAKEDA 1981. Ordinary chondrite parent body: An internal heating model. *Proc. Lunar Planet. Sci. Conf., 12B,* 1145–1152.

OLSEN, E. J., A. M. DAVIS, I. D. HUTCHEON, R. N. CLAYTON, T. K. MAYEDA, AND L. GROSSMAN 1988. Murchison xenoliths. *Geochim. Cosmochim. Acta* 52, 1615–1626.

PATTERSON, C., AND D. SPAUTE 1988. Self-termination of runaway growth in the asteroid belt (abstract). Papers presented at Asteroids II Conference, Tucson, AZ.

PRINN, R. G., AND B. FEGLEY, JR. 1989. Solar nebula chemistry: Origin of planetary, satellite, and cometary volatiles. In *Origin and Evolution of Planetary and Satellite Atmospheres* (S. Atreya, J. Pollack, and M. Matthews, Eds.). Univ. of Arizona Press, Tucson, in press.

REYNOLDS, R. T., P. E. FRICKER, AND A. L. SUMMERS 1966. Effects of melting upon thermal models of the Earth. *J. Geophys. Res.* 71, 573–582.

RICHARDSON, S. M. (1978). Vein formation in the CI carbonaceous chondrites. *Meteoritics* 13, 141–159.

RIETMEIJER, F. J. M., AND I. R. D. MACKINNON 1985. Poorly graphitized carbon as a new cosmothermometer for primitive extraterrestrial materials. *Nature* 315, 733–736.

ROBIE, R. A., AND D. R. WALDBAUM 1968. Thermodynamic properties of minerals and related substances at 298.15°K and one atmosphere (1.013 bars) pressure and at high temperatures. *U.S. Geol. Survey Bull.,* 1259.

SAFRONOV, V. S. 1972. *Evolution of the Protoplanetary Cloud and Formation of the Earth and the Planets.* Nauka, Moscow. [Translated from the Russian, *NASA Tech. Trans., F-677*].

SAFRONOV, V. S. 1978. The heating of the Earth during its formation. *Icarus* 33, 1–12.

SAFRONOV, V. S. 1979. On the origin of asteroids. In *Asteroids* (T. Gehrels, Ed.), pp. 975–991. Univ. of Arizona Press, Tucson.

SCHATZ, J. F., AND G. SIMMONS 1972. Thermal conductivity of Earth materials at high temperatures. *J. Geophys. Res.* 77, 6966–6983.

SCHUBERT, G., P. CASSEN, AND R. E. YOUNG (1979). Subsolidus convective cooling histories of terrestrial planets. *Icarus* 38, 192–211.

SCOTT, E. R. D., AND R. S. RAJAN 1981. Metallic minerals, thermal histories, and parent bodies of some xenolithic, ordinary chondrites. *Geochim. Cosmochim. Acta* 45, 53–67.

SEARS, D. W., J. R. ASHWORTH, C. P. BROADBENT, AND A. W. R. BEVAN 1984. Studies of an artificially shock-loaded H group chondrite. *Geochim. Cosmochim. Acta* 48, 343–360.

SHARPE, H. N., AND W. R. PELTIER 1978. Parameterized convection and the Earth's thermal history. *Geophys. Res. Lett.* 5, 737–740.

SKINNER, W. R. 1989. Compaction and lithification of chondrites (abstract). In *Lunar and Planetary Science XX,* pp. 1020–1021. Lunar and Planetary Institute, Houston, TX.

SNEYD, D. S., H. Y. McSWEEN, JR., N. SUGIURA, D. W. STRANGWAY, AND G. L. NORD, JR. 1988. Origin of petrofabric and magnetic anisotropy in ordinary chondrites. *Meteoritics* 23, 139–149.

SONETT, C. P., D. S. COLBURN, K. SCHWARTZ, AND K. KEIL 1970. The melting of asteroidal-sized bodies by unipolar dynamo induction from a primordial T-Tauri sun. *Astrophys. Space Sci.* 7, 446–488.

SONETT, C. P., AND R. T. REYNOLDS 1979. Primordial heating of asteroidal parent bodies. In *Asteroids* (T. Gehrels, Ed.), pp. 822–848. Univ of Arizona Press, Tucson.

STRAUS, J. M. 1974. Large amplitude convection in porous media. *J. Fluid Mech.* 64, 51–63.

STRAUS, J. M., AND G. SCHUBERT 1977. Thermal convection of water in a porous medium: Effects of temperature- and pressure-dependent thermodynamic and transport properties. *J. Geophys. Res.* 82, 325–333.

SUGIURA, N., AND D. W. STRANGWAY 1983. Magnetic

anisotropy and porosity of chondrites. *Geophys. Res. Lett.* **10**, 83–86.

SUGIURA, N., N. S. BRAR, D. W. STRANGWAY, AND T. MATSUI 1984. Degassing of meteorite parent bodies. *Proc. Lunar Planet. Sci. Conf. 14th, J. Geophys. Res.* **89**, *Suppl.*, B641–B644.

THURBER, C. H., A. T. HSUI, AND M. N. TOKSOZ 1980. Thermal evolution of Ganymede and Callisto: Effects of solid-state convection and constraints from Voyager imagery. *Proc. Lunar. Planet. Sci. Conf. 11th*, 1957–1977.

TOMEOKA, K., AND P. R., BUSECK 1985. Indicators of aqueous alteration in CM carbonaceous chondrites: Microtextures of a layered mineral containing Fe, S, O, and Ni. *Geochim. Cosmochim. Acta* **49**, 2149–2163.

TOMEOKA, K. AND P. R. BUSECK 1988. Matrix mineralogy of the Orgueil CI carbonaceous chondrite. *Geochim. Cosmochim. Acta* **52**, 1627–1640.

TOULOUKIAN, Y. S., P. E. LILEY, AND S. C. SAXENA 1970. *Thermophysical Properties of Matter*, Vol. 3. IFI/Plenum, New York.

TOULOUKIAN, Y. S., AND MAKITA 1970. *Thermophysical Properties of Matter*, Vol. 6. IFI/Plenum, New York.

TOULOUKIAN, Y. S., S. C. SAXENA, AND P. HESTERMANS 1975. *Thermophysical Properties of Matter*, Vol. 11. IFI/Plenum, New York.

TURCOTTE, D. L., F. A. COOKE, AND R. J. WILLEMANN 1979. Parameterized convection within the moon and terrestrial planets. *Proc. Lunar. Sci. Conf. 10th*, 2375–2392.

TURCOTTE, D. L., AND G. SCHUBERT 1982. *Geodynamics*. Wiley, New York.

VEEDER, G. J. 1986. The IRAS asteroid data. In *IRAS Asteroid and Comet Survey, Preprint Version No. 1* (D. L. Matson, Ed.), Vol. 2, Nos. 1, 2, p. 54. Internal Document D-3698, Jet Propulsion Laboratory, Pasadena, CA.

WASHBURN, E. W. 1928. Vapor pressure of ice and water <100°C. In *International Critical Tables*, Vol. 3. (E. W. Washburn, Ed.), pp. 210–212. McGraw–Hill, New York.

WASSON, J. T., AND G. W. WETHERILL 1979. Dynamical, chemical, and isotopic evidence regarding the formation locations of asteroids and meteorites. In *Asteroids* (T. Gehrels, Ed.), pp. 926–974. Univ. of Arizona Press, Tucson.

WEGNER, W. W., AND W. G. ERNST 1983. Experimentally determined hydration and dehydration reaction rates in the system $MgO-SiO_2-H_2O$. *Amer. J. Sci. Ser. A* **238**, 151–180.

WETHERILL, G. W. 1980. Formation of the terrestrial planets. *Annu. Rev. Astron. Astrophys.* **18**, 77–113.

WOOD, J. A., AND G. E. MORFILL 1988. A review of solar nebula models. In *Meteorites and the Early Solar System* (J. F. Kerridge and M. S. Matthews, Eds.), pp. 329–347. Univ. of Arizona Press, Tucson.

YOMOGIDA, K., AND T. MATSUI 1983. Physical properties of ordinary chondrites. *J. Geophys. Res.* **88**, 9513–9533.

YOMOGIDA, K., AND T. MATSUI 1984. Multiple parent bodies of ordinary chondrites. *Earth Planet. Sci. Lett.* **68**, 34–42.

ZEMANSKY, M. W., AND R. H. DITTMAN 1981. *Heat and Thermodynamics*. McGraw–Hill, New York.

ZOLENSKY, M. E., R. A. BARRETT, AND M. PRINZ 1989. Petrography, mineralogy, and matrix composition of Yamato-82162, a new CI2 chondrite (abstract). In *Lunar and Planetary Science XX*, pp. 1253–1254. Lunar and Planetary Institute, Houston, TX.

ZOLENSKY, M. E., AND H. Y. MCSWEEN, JR. 1988. Aqueous alteration. In *Meteorites and the Early Solar System*. (J. F. Kerridge and M. S. Matthews, Eds.), pp. 114–143. Univ. of Arizona Press, Tucson.